Analysis of a pan-cancer panel reveals the amino acid metabolism-related gene MTHFD1 as a potential prognostic and immunotherapeutic biomarker

SHUNSONG GONG[1], JIAXUE YANG[2], CHAO PAN[3], FENGLAN PENG[4] and CHUAN PAN[5]

[1]Department of Thoracic Surgery, Yangxin People's Hospital, Huangshi, Hubei 435200, P.R. China; [2]Third Clinical Medical College, Nanchang University, Nanchang, Jiangxi 330006, P.R. China; [3]Department of Respiratory Medicine, Yangxin People's Hospital, Huangshi, Hubei 435200, P.R. China; [4]Department of Otolaryngology, Hubei No. 3 People's Hospital of Jianghan University, Wuhan, Hubei 430033, P.R. China; [5]Department of Nephrology and Endocrinology, Yangxin People's Hospital, Huangshi, Hubei 435200, P.R. China

Received April 4, 2024; Accepted April 23, 2025

DOI: 10.3892/etm.2025.12892

Abstract. Methylenetetrahydrofolate dehydrogenase 1 (MTHFD1) serves a role in amino acid metabolism and may influence tumor progression. However, to the best of our knowledge, a comprehensive analysis of MTHFD1 in various types of cancer has not been previously performed. Therefore, the present study aimed to investigate the expression profile and prognostic implication of MTHFD1 across various types of cancer, whilst assessing its potential as a novel biomarker and therapeutic target. The expression of MTHFD1 in tissues from various types of cancer was analyzed using online tools based on data from the Cancer Cell Line Encyclopedia and Clinical Proteomic Tumor Analysis Consortium, as well as in-house differential expression analysis using data from The Cancer Genome Atlas (TCGA). The association between MTHFD1 and prognosis was investigated using Kaplan-Meier survival analysis and Cox proportional hazards regression analysis based on TCGA datasets. Furthermore, the association between MTHFD1 and the tumor microenvironment (TME) was investigated using the 'estimation of stromal and immune cells in malignant tumor tissues using expression data' and 'cell-type identification by estimating relative subsets of RNA transcripts' algorithms. The correlation between MTHFD1 expression and tumor mutational burden (TMB), microsatellite instability (MSI) or 48 immune checkpoint blockade-related gene expression levels was investigated using Pearson correlation analyses. The predictive potential of MTHFD1 for immunotherapy efficacy was evaluated using the tumor immune dysfunction and exclusion (TIDE) algorithm with the IMvigor210 dataset. Subsequently, the effects of MTHFD1 on the proliferation and invasion of A549 and 786-O cell lines were assessed using colony formation and Transwell assays. Analysis across 33 tumor types revealed that MTHFD1 expression was significantly upregulated in 12 cancers (e.g., bladder urothelial carcinoma) and downregulated in 6 cancers (e.g., breast invasive carcinoma). Moreover, high MTHFD1 expression was associated with a poorer prognosis in kidney chromophobe and lung adenocarcinoma, but with better prognosis in kidney renal clear cell carcinoma. Additionally, the activity of MTHFD1, evaluated using the single-sample Gene Set Enrichment Analysis algorithm, was significantly upregulated in 21 cancer types, including bladder urothelial carcinoma and breast invasive carcinoma, compared with corresponding normal tissues. MTHFD1expression levels were negatively correlated with immune cell infiltration in 16 tumor types [e.g., adrenocortical carcinoma (ACC)] and positively correlated only in uveal melanoma (UVM). Additionally, MTHFD1 expression levels showed significant correlations with TMB in 17 tumors (e.g., ACC), were negatively correlated with TIDE scores in most tumors except mesothelioma, liver hepatocellular carcinoma, diffuse large B-cell lymphoma and cholangiocarcinoma, and were associated with MSI in 9 tumor types (e.g., UVM). Multivariant Cox regression analysis revealed that MTHFD1 expression was an independent risk factor for prognosis in lung adenocarcinoma, whilst it was an independent protective factor in clear cell renal cell carcinoma, highlighting its distinct prognostic roles in these two tumor types. *In vitro* experiments found that knocking down or overexpressing MTHFD1 in A549 and 786-O cells, respectively, reduced the corresponding malignant phenotypes. Overall, to the best of our knowledge, results of the present study provided the first comprehensive analysis of MTHFD1 as a potential cancer biomarker and highlighted its role in immune suppression within the TME. These findings suggested that targeting MTHFD1 may be a novel therapeutic strategy, which may enhance the efficacy of immunotherapy and improve the outcomes of patients with various types of cancer.

Correspondence to: Dr Chuan Pan, Department of Nephrology and Endocrinology, Yangxin People's Hospital, 81 Ruxue Road, Huangshi, Hubei 435200, P.R. China
E-mail: panchuanyxrmyy@163.com

Key words: methylenetetrahydrofolate dehydrogenase 1, prognostic, immunotherapeutic, biomarker, pan-cancer

Introduction

By 2040, the global number of patients to be newly diagnosed with cancer is estimated to be 28.4 million, representing a 47% increase from 2020 (1). This substantial rise in incidence is a notable threat to human health and survival, which is an economic burden on society. Despite advances in personalized and precision cancer therapies, several challenges remain. The lack of sensitive early diagnostic biomarkers results in ~52.8% of patients being diagnosed already with advanced stage cancer on first presentation (2). Additionally, a proportion of patients will experience recurrence and metastasis even after comprehensive treatment, leading to 5-year survival rates of <50% for several types of cancer (2). For instance, in head and neck squamous cell carcinoma (HNSC), ~50.6% of recurrences occur within 6 months post-treatment, with 88.6% occurring within 2 years (3). Similarly, patients with colorectal cancer face a 5-year recurrence rate of ~26.9%, with survival rates dropping significantly in advanced stages (4). These issues underscore the importance of identifying early diagnostic biomarkers whilst also elucidating the molecular and cellular mechanisms underlying tumor progression.

During cancer development, the reprogramming of amino acid metabolism is an important process (5). Numerous studies have demonstrated the role of amino acid metabolic reprogramming in the malignant progression of cancer cells (5-7). Upregulation of the cysteine/glutamate transporter 2 (ASCT2) has been reported to promote glutamine uptake in colon cancer and lung adenocarcinoma cells, thereby creating a cycle of abnormal proliferation (8). In HNSC and triple-negative basal-like breast cancer xenograft models, knocking down ASCT2 was found to reduce the activity of mTOR complex 1 to inhibit tumor growth (9-11). Additionally, in colorectal cancer cells, activating mutations in the KRAS gene, particularly the common G12D and G13D variants, reprogram cellular metabolism by enhancing glutamine uptake (12). This occurs through upregulation of glutamine transporters and increased glutaminolysis, providing intermediates for the tricarboxylic acid cycle to support tumor growth (13). Additionally, the L-type amino acid transporter 1 (LAT1), encoded by SLC7A5, is often overexpressed in colorectal cancer cells (13). LAT1 facilitates the uptake of essential amino acids such as leucine, which activates the mTOR signaling pathway, thereby promoting protein synthesis and cell proliferation (14). Blocking the cystine antiporter solute carrier family 7 member 11/glutathione axis selectively can also inhibits the proliferation of KRAS-mutant non-small cell lung cancer (15,16). These aforementioned findings suggest that targeting amino acid metabolism may be a potentially viable therapeutic option, but currently there is a lack of research in this area.

Methylenetetrahydrofolate dehydrogenase 1 (MTHFD1) is an important regulatory factor in the progression of various types of cancer, including gallbladder, pancreatic, metastatic colorectal and non-small cell lung cancers (17-20). Over the past decade, its association with amino acid metabolism has been garnering attention in the field of cancer research. In pancreatic cancer, MTHFD1 was found to be activated by decrotonylation at the Lys354 and Lys553 sites, which enhances resistance to ferroptosis and promotes cancer development (21). MTHFD1 mainly participate in one-carbon metabolism, regulating the metabolism of several amino acids, particularly serine, glycine, histidine, methionine, tryptophan and lysine (22-25). By modulating the metabolism of these amino acids, MTHFD1 can in turn regulate nucleic acid synthesis, methylation reactions, protein modification and cell proliferation (26). Since these four pathways are important for the proliferation of tumor cells (27-30), MTHFD1 may yet serve a key role in cancer progression through its regulation of amino acid metabolism. Therefore, MTHFD1 may have value as a therapeutic target against cancer. However, to the best of our knowledge, the specific roles of MTHFD1 in various types of cancer are yet to be elucidated, highlighting a gap in the latest research field.

Therefore, the present study aimed to fill this gap using the Cancer Cell Line Encyclopedia (CCLE) database, the Clinical Proteomic Tumor Analysis Consortium (CPTAC), The Cancer Genome Atlas (TCGA) and the Genotype-Tissue Expression (GTEx) project to investigate the expression patterns, prognostic value and correlations of MTHFD1 with immune cell infiltration in several types of cancer. The predictive performance of MTHFD1 expression levels on immunotherapy outcomes was also investigated. Additionally, *in vitro* cell experiments were used to investigate the role of MTHFD1 in lung adenocarcinoma (LUAD) and clear cell renal cell carcinoma (KIRC) and to further examine its molecular mechanisms in cancer progression.

Materials and methods

Data retrieval. mRNA expression matrices, clinical information, survival data and tumor mutational burden (TMB) for 33 types of tumor were obtained from TCGA (https://www.cancer.gov/tcga) and the GTEx (https://gtexportal.org/home/) databases. The TCGA data were accessed using the UCSC Xena platform (https://xenabrowser.net/) by searching for 'TCGA Pan-Cancer' datasets. RNA-seq data (HTSeq-FPKM format) and corresponding clinical information were downloaded. Samples lacking survival information were excluded. The GTEx data were obtained from the GTEx Portal (v8 release), selecting normal tissues anatomically corresponding to the tumor tissues under study. RNA-seq transcripts per million data were used. The 'IMvigor210' dataset, consisting of RNA-sequencing data and clinical information from patients with metastatic urothelial carcinoma treated with atezolizumab, was accessed from the website (http://research-pub.Gene.com/imvigor210corebiologies). Additionally, MTHFD1 mRNA expression data in tumor cells was obtained from the CCLE (https://sites.broadinstitute.org/ccle) database, using the keyword 'MTHFD1'. MTHFD1 protein expression levels in tumor and normal tissues across 10 types of cancer were further validated using the 'CPTAC analysis' module of the University of Alabama at Birmingham Cancer Data Analysis Portal (http://ualcan.path.uab.edu/analysis-prot.html). Fig. 1 presents a flowchart of the present study.

Immunological analysis. The 'estimation of stromal and immune cells in malignant tumor tissues using expression data' (ESTIMATE) R package (version 1.0.13) (31) was used to compute the tumor microenvironment (TME) status, including the stromal score, immune score and ESTIMATE

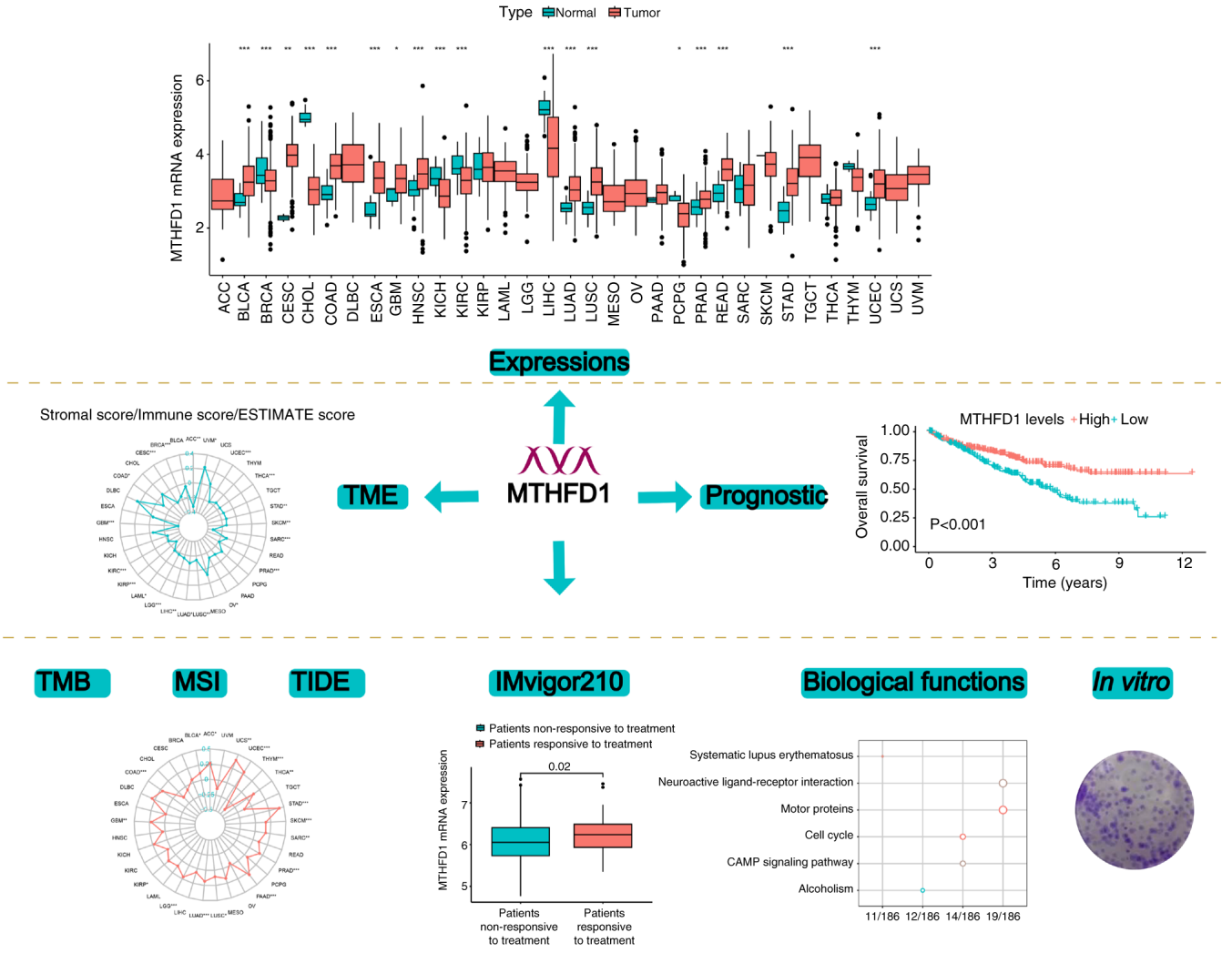

Figure 1. Flow chart of the progression of experiments used in the present study. MTHFD1, methylenetetrahydrofolate dehydrogenase 1; TME, tumor microenvironment; ESTIMATE, estimation of stromal and immune cells in malignant tumor tissues using expression data; TMB, tumor mutational burden; MSI, microsatellite instability; TIDE, tumor immune dysfunction and exclusion.

score, across 33 types of cancer using RNA-seq data obtained from TCGA. Additionally, the cell-type identification by estimating relative subsets of RNA transcripts (CIBERSORT) algorithm (32) was used to calculate the abundance of the different immune cell infiltrates. Microsatellite instability (MSI) and tumor immune dysfunction and exclusion (TIDE) scores were determined using the TIDE website (http://tide.dfci.harvard.edu/), with all analyses performed using the default parameters. Radar plots depicting associations with MTHFD1 expression were generated using the 'fmsb' package (version 0.7.6) (https://CRAN.R-project.org/package=fmsb).

Biological function analysis. The activity of MTHFD1 was assessed using the single sample gene set enrichment analysis (ssGSEA) algorithm implemented through the 'GSVA' (version 1.48.0) (33) and 'GSEABase' (version 1.62.0) packages (https://bioconductor.org/packages/GSEABase). To explore the biological pathways potentially regulated by MTHFD1, differentially expressed genes (DEGs) between the high and low MTHFD1 expression groups were identified using the 'limma' package (version 3.56.1) (34), with an absolute log2 fold-change >0.585 and a false discovery rate <0.05 as the cutoff thresholds. Subsequently, Gene Ontology (GO) and Kyoto Encyclopedia of Genes and Genomes (KEGG) enrichment analyses were performed using the 'clusterProfiler' package (version 4.4.1) (35) to elucidate the functional roles of these DEGs. In these analyses, terms and pathways were considered significantly enriched if the adjusted P-value was <0.05, indicating that the enrichment was statistically significant after correcting for multiple testing.

Cell culture and transfection. The LUAD cell line A549 and the KIRC cell line 786-O were purchased from the American Type Culture Collection. Cells were cultured in RPMI-1640 medium (MilliporeSigma) supplemented with 10% FBS (Thermo Fisher Scientific, Inc.) and 1% penicillin and streptomycin. The cells were maintained at 37°C with 5% CO_2 in a humidified incubator. During culture, the medium was refreshed every 2-3 days or as needed to ensure optimal growth conditions. Cells were passaged upon reaching ~80% confluence. Following the manufacturer's protocol, cells were transfected with a negative control (NC)-overexpression (OE) vector [empty pLV-CMV-MCS-PGK-Puro; OBiO Technology (Shanghai) Corp., Ltd.] or an OE-MTHFD1 [lentiviral vector

backbone: pLV-CMV-MCS-PGK-Puro; OBiO Technology (Shanghai) Corp., Ltd.]. For gene knockdown experiments, cells were transfected with NC-small interfering (si)RNA or si-MTHFD1 [both OBiO Technology (Shanghai) Corp., Ltd.]. Lipo8000™ (Beyotime Institute of Biotechnology) was used for both plasmids (including lentiviral vectors) and siRNAs. For lentiviral vector transfection during packaging, 2 μg of plasmid DNA was used per well. For siRNA transfection, 50 nM siRNA was used per well. Lentiviral infection was performed by incubating cells with viral particles in the presence of Polybrene (5-8 μg/ml). Transfected or infected cells were incubated at 37˚C with 5% CO_2 for 48 h. After confirming transfection efficiency by western blot analysis, cells were used for subsequent experiments, typically at 24-48 h post-transfection, depending on the specific requirements of the experiments. The specific sequences of the constructs are shown in Table SI.

Western blotting. Proteins from cells were extracted using RIPA buffer (Cell Signaling Technology, Inc.). Equal amounts of protein were loaded, separated using SDS-PAGE and then transferred onto PVDF membranes. The protein concentration was determined using the bicinchoninic acid assay. The mass of protein loaded per lane was 20 μg. The SDS-PAGE gel used was a 10% polyacrylamide gel. The membranes were blocked with 5% non-fat milk in TBST (containing 0.1% Tween-20) for 1.5 h at room temperature. Subsequently, the membranes were incubated overnight at 4˚C with primary antibodies against MTHFD1 (1:2,000; cat. no. ab226341; Abcam) or GAPDH (1:10,000; cat. no. ab263962; Abcam) following the manufacturer's protocol. After washing with TBST (containing 0.1% Tween-20), the membranes were incubated with a secondary Goat Anti-Rabbit IgG H&L (HRP) antibody (1:4,000; cat. no. ab6721; Abcam) for 2 h at room temperature. Following additional washes with TBST(containing 0.1% Tween-20), protein bands were visualized using ECL chemiluminescence (cat. no. 34580; Thermo Fisher Scientific, Inc.), followed by imaging and semi-quantification of the protein expression levels using Image Studio Lite software (version 5.0) (LI-COR Biosciences).

Colony formation assay. Following the aforementioned treatments, cells were trypsinized and seeded into 6-well plates at a density of 500 cells/well and incubated at 37˚C with 5% CO_2 for 14 days, with the media being changed every 2-3 days to ensure optimal growth conditions. After incubation, the cells were fixed with 4% paraformaldehyde at room temperature for 15 min and stained with crystal violet at room temperature for 30 min. After washing with phosphate-buffered saline (PBS), colony formation was observed under an inverted phase-contrast light microscope, and the number of colonies was counted manually using visual inspection. Colonies were defined as clusters of >50 cells.

Transwell migration assays. A Transwell migration assay was used to assess the migration of cells. Cells in the logarithmic growth phase were harvested and digested with trypsin. The cells were resuspended in serum-free DMEM medium and adjusted to a density of $1x10^5$ cells/ml. A total of 200 μl of the cell suspension was added to the upper chamber of the Transwell insert (8 μm pore size), whilst 500 μl supplemented DMEM was added to the lower chamber. The DMEM was supplemented with 10% FBS and 1% penicillin-streptomycin. The cells were incubated at 37˚C with 5% CO_2 for 48 h. After incubation, the Transwell inserts were removed and the cells on the membrane were fixed with 4% paraformaldehyde at room temperature for 15 min. Subsequently, the cells were stained with 0.1% crystal violet solution at room temperature for 15 min and then washed with PBS to remove residual crystal violet. Cells in the upper chamber of the Transwell membrane that had not migrated were removed using a cotton swab, whereas migratory cells in the lower chamber were counted manually using a light microscope.

Statistical analysis. *In vitro* experiments were repeated three times. In the bioinformatics analysis, comparisons of the MTHFD1 expression levels between two groups was performed using the Wilcoxon rank-sum test. For comparisons involving three or more groups, the Kruskal-Wallis test was used, followed by the Bonferroni post hoc test for significant results. For the *in vitro* experiments, the mean ± standard deviation values of the different groups were compared using one-way ANOVA. When significant differences were found, the least significant difference post hoc test was used for pairwise comparisons. Pearson correlation analysis was used for correlation analysis. The prognostic value of MTHFD1 expression levels in tumors was investigated using univariate Cox regression analysis. Kaplan-Meier (KM) survival curves for patients in each group were produced, and comparisons were performed using log-rank tests. Additionally, multivariate Cox regression analysis was performed to evaluate the independent prognostic value of MTHFD1 expression levels, adjusting for potential confounding factors such as age, sex and clinical stage. $P<0.05$ was considered to indicate a statistically significant difference. All statistical analyses were performed using R software (version 4.2.1; The R Foundation for Statistical Computing) and GraphPad Prism (version 9.5.1; Dotmatics).

Results

MTHFD1 exhibits differential expression in 33 types of tumors. An analysis of the MTHFD1 mRNA expression levels across 33 types of tumor was performed. The results revealed significant differences in the MTHFD1 expression levels between 18 tumors and their normal tissue counterparts. Specifically, MTHFD1 was upregulated in the tumor tissues of bladder urothelial carcinoma (BLCA), cervical squamous cell carcinoma (CESC), colon adenocarcinoma (COAD), esophageal carcinoma (ESCA), glioblastoma multiforme (GBM), HNSC, LUAD, lung squamous cell carcinoma (LUSC), prostate adenocarcinoma (PRAD), rectum adenocarcinoma (READ), stomach adenocarcinoma (STAD) and uterine corpus endometrial carcinoma (UCEC). However, the expression of MTHFD1 was downregulated in breast invasive carcinoma (BRCA), cholangiocarcinoma (CHOL), kidney chromophobe (KICH), KIRC, liver hepatocellular carcinoma (LIHC) and pheochromocytoma and paraganglioma (PCPG) (Fig. 2A). Additionally, across all tumor tissues, LIHC exhibited the highest expression level of MTHFD1, whereas PCPG had the lowest (Fig. 2B). Furthermore, using the ssGSEA algorithm, it was observed

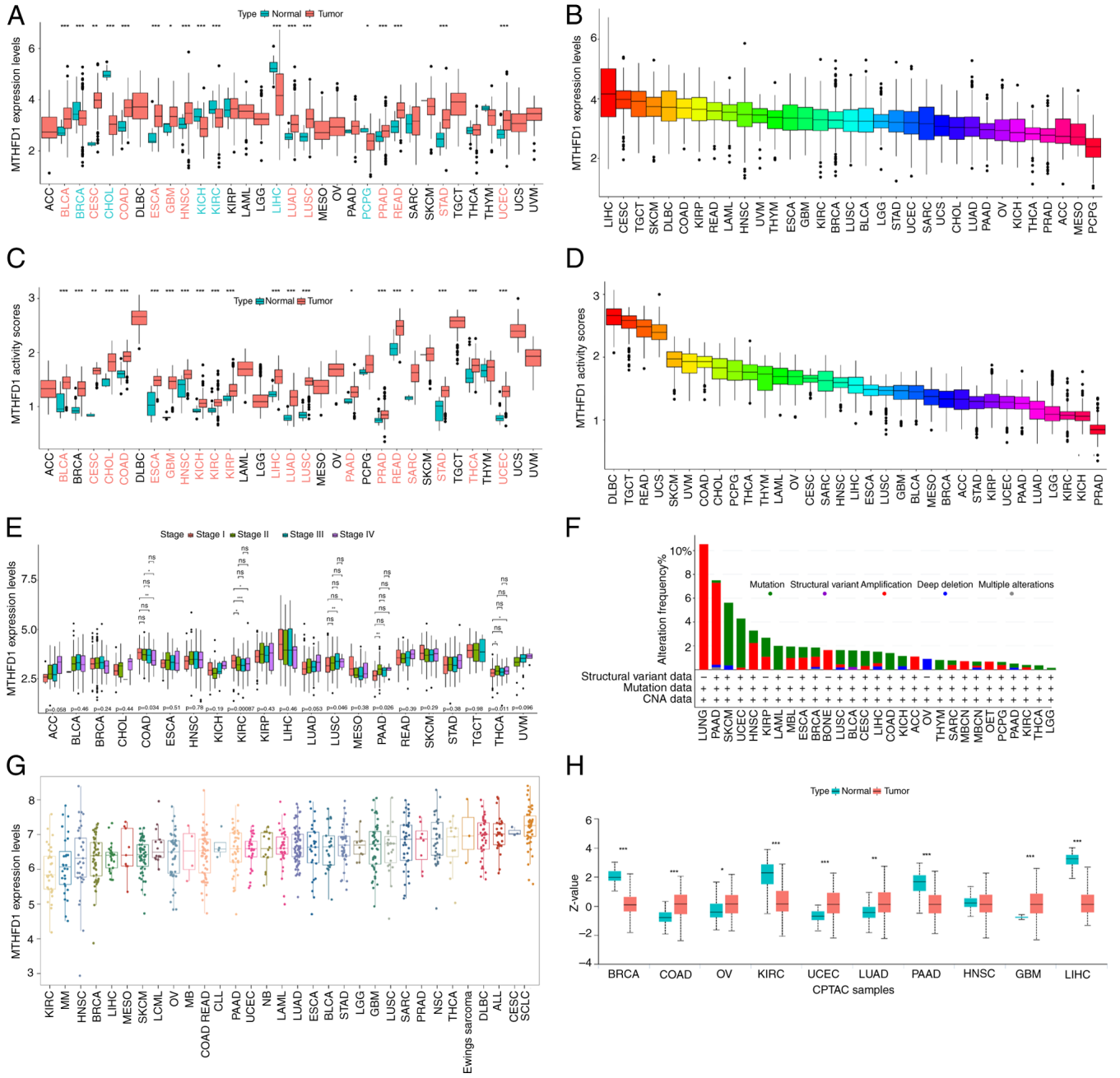

Figure 2. Analysis of MTHFD1 mRNA expression levels, activity and alterations across 33 types of cancer. (A) Boxplots showing MTHFD1 mRNA expression levels in tumor tissues compared with normal tissues across different types of cancer. (B) Comparison of MTHFD1 mRNA expression levels across different types of cancer. (C) Boxplots indicating the MTHFD1 activity levels, as determined by the ssGSEA algorithm, in tumor tissues compared with normal tissues across different types of cancer. (D) Distribution of MTHFD1 activity, as determined by the ssGSEA algorithm, across different types of tumor. (E) MTHFD1 mRNA expression levels across different clinical stages in different types of tumor. (F) Bar graph showing the frequency of alterations in MTHFD1 within different types of cancer. (G) MTHFD1 expression levels across different cancer cell lines. (H) Comparison of MTHFD1 expression levels between tumor and normal tissues in the CPTAC dataset. *P<0.05, **P<0.01 and ***P<0.001. For certain cancer types (e.g., ACC, UCS, UVM), the 'normal' MTHFD1 expression levels are not shown as these data are not available in the TCGA database used for analysis. MTHFD1, methylenetetrahydrofolate dehydrogenase 1; ACC, adrenal carcinoma; BLCA, bladder urothelial carcinoma; BRCA, breast invasive carcinoma; CESC, cervical squamous cell carcinoma; CHOL, cholangiocarcinoma; COAD, colon adenocarcinoma; DLBC, diffuse large B-cell lymphoma; ESCA, esophageal carcinoma; GBM, glioblastoma multiforme; HNSC, head and neck squamous cell carcinoma; KIRC, kidney renal clear cell carcinoma; KIRP, kidney renal papillary cell carcinoma; LGG, low-grade glioma; LIHC, liver hepatocellular carcinoma; LUAD, lung adenocarcinoma; LUSC, lung squamous cell carcinoma; OV, ovarian serous cystadenocarcinoma; PAAD, pancreatic adenocarcinoma; PCPG, pheochromocytoma and paraganglioma; PRAD, prostate adenocarcinoma; READ, rectum adenocarcinoma; SARC, sarcoma; SKCM, skin cutaneous melanoma; STAD, stomach adenocarcinoma; TGCT, testicular germ cell tumors; THCA, thyroid carcinoma; THYM, thymoma; UCEC, uterine corpus endometrial carcinoma; UVM, uveal melanoma; CAN, copy number alteration; CTPA, CPTAC dataset for protein expression in cancer; ssGSEA, single-sample gene set enrichment analysis; Z-Score, standardized value for the data points.

that MTHFD1 activity (enrichment score) was increased in 21 tumor tissues compared with normal tissues (including BLCA and BRCA; Fig. 2C). No tumors showed a significant decrease. Additionally, diffuse large B-cell lymphoma (DLBC) had the highest MTHFD1 activity and PRAD the lowest across all of the tumors investigated (Fig. 2D). Variations in the MTHFD1

expression levels were also observed across different clinical stages in COAD, KIRC, LUSC, pancreatic adenocarcinoma (PAAD) and thyroid carcinoma (THCA; Fig. 2E). Specifically, in COAD, the MTHFD1 expression level of stage I was significantly increased compared with that of stage IV. Additionally, in KIRC, the MTHFD1 expression level of stage I was significantly higher compared with that of stages II, III and IV. However, in LUSC, PAAD and THCA, the MTHFD1 expression levels of stage I were markedly lower compared with those of stage II (Fig. 2E). Using the cBioPortal database, the distribution of MTHFD1 mutations across various tumors was next investigated, where skin cutaneous melanoma (SKCM) was revealed to have the highest mutational frequency (Fig. 2F). As shown in Fig. 2G, the expression of MTHFD1 was found to be the lowest in KIRC cell lines and highest in small cell lung cancer cell lines. Furthermore, data from the CPTAC database indicated that the expression level differences in MTHFD1 between tumor and normal tissues in BRCA, COAD, KIRC, UCEC, LUAD, GBM and LIHC were consistent with the data from TCGA (Fig. 2H). In summary, these findings demonstrate the diverse expression patterns of MTHFD1 across different tumors, suggesting differences in its role and the potential for further research.

MTHFD1 exhibits prognostic value in 33 types of tumors. Subsequently, the prognostic values of MTHFD1 expression levels in various tumors were investigated. Univariate Cox regression analysis revealed that MTHFD1 was identified as a prognostic factor for overall survival (OS) in adrenocortical carcinoma (ACC), KICH, KIRC, LUAD, mesothelioma (MESO), PAAD, PCPG and uveal melanoma (UVM; Fig. 3A). KM survival analysis was performed to assess the association between MTHFD1 expression and survival outcomes. Only cancer types with statistically significant differences ($P<0.05$) in the KM analysis were included for visualization, independent of the univariate Cox regression results. Patients with low MTHFD1 expression levels had an increased OS compared with those with high MTHFD1 expression levels in ACC, KICH, LUAD, PAAD, PCPG and UVM. However, the opposite was demonstrated in CESC, KIRC, STAD and thymoma (THYM; Fig. 3B-K).

Results of progression-free survival (PFS) analysis indicated that MTHFD1 expression was associated with PFS in ACC, KICH, KIRC, LUAD, MESO, PAAD, SARC, STAD, THCA and UVM (Fig. 4A). KM curves demonstrated that patients with low MTHFD1 expression levels had a longer PFS compared with those with high expression levels in ACC, KICH, LUAD, SARC, THCA and UVM. However, the opposite was revealed in KIRC and STAD (Fig. 4B-I).

Subsequent disease-specific survival (DSS) analysis revealed that, excluding CESC and THYM, which were not significantly associated with OS or DSS, the survival trends for other cancer types were consistent with those observed for OS. Furthermore, in COAD, patients with high MTHFD1 expression levels had a longer DSS rate compared with those with low expression levels (Fig. 5A-J).

Taken together, although the expression levels of MTHFD1 may have prognostic value in various types of tumors, consistent results between the Kaplan-Meier and Cox regression analyses are only demonstrated for a subset of tumors. For example, for OS, consistent results were indicated for ACC, KICH, KIRC, LUAD, PAAD, PCPG and UVM. In addition, for PFS, consistent results were revealed for ACC, KICH, KIRC, LUAD, SARC, STAD, THCA and UVM. Additionally, for DSS, consistent findings were demonstrated for KICH, KIRC, LUAD, PAAD, PCPG, STAD and UVM. These consistent results between the Kaplan-Meier and Cox regression analyses suggested that the expression level of MTHFD1 may be reliable as a prognostic marker in these types of tumors, indicating its potential utility in clinical decision-making.

MTHFD1 exhibits potential inhibition of immune cell infiltration in 33 types of tumors. Given the differential expression of MTHFD1 across the various tumors and its potential prognostic value, coupled with the important role of the TME in tumor progression (36), the association between MTHFD1 expression levels and immune cell infiltration was further analyzed using multiple algorithms. The ESTIMATE algorithm indicated a negative correlation between MTHFD1 expression levels and stromal score in 21/33 types of tumor, excluding UVM, USC, PCPG, PAAD, MESO, LIHC, LAML, KICH, esophageal adenocarcinoma (ESAC), DLBC, CHOL, and BLCA (Fig. 6A). Additionally, there was a negative correlation between MTHFD1 expression levels and immune cell infiltration in 16/33 types of tumor (such as ACC, UCEC, THCA and SKCM) and a positive correlation only in UVM (Fig. 6B). The ESTIMATE score was positively correlated with UVM, whereas it was negatively correlated in 19/33 types of tumor (such as ACC and UCEC; Fig. 6C). This suggested that an increased MTHFD1 expression level may inhibit immune cell activity in the majority of tumors. Further analysis using the CIBERSORT algorithm revealed a negative correlation between MTHFD1 expression levels and the infiltration abundance of the majority of immune cell types. For example, in COAD, MTHFD1 expression was positively correlated with the infiltration abundance of resting mast cells and M1 macrophages, while in UCEC, it was positively correlated with $CD8^+$ T cells. By contrast, in KIRC and LGG, MTHFD1 expression levels showed a negative correlation with $CD8^+$ T cell infiltration. Additionally, MTHFD1 was negatively correlated with pro-tumor immune cells, such as regulatory T cells (Tregs), but positively correlated with antitumor immune cells, including M1 macrophages (Fig. 6D). In summary, the findings from multiple algorithms indicated that high MTHFD1 expression levels may suggest an immunosuppressive state, whilst low expression levels may indicate immune activation. This highlighted a possible potential for MTHFD1 in tumor immunology research.

MTHFD1 as a potential biomarker for predicting immunotherapy efficacy in 33 types of tumors. Immunotherapy, as a relatively non-invasive treatment modality, has potential in tumor management. However, its clinical application is notably hindered due to a lack of efficacy in 60-80% of patients with solid tumors (37,38). Therefore, there is value in identifying effective predictive biomarkers for immunotherapy response. In 2020, TMB received Food and Drug Administration (FDA) approval for use as a biomarker to guide the selection of treatments for patients with solid tumors exhibiting high TMB (39). Therefore, the association between MTHFD1 and TMB was

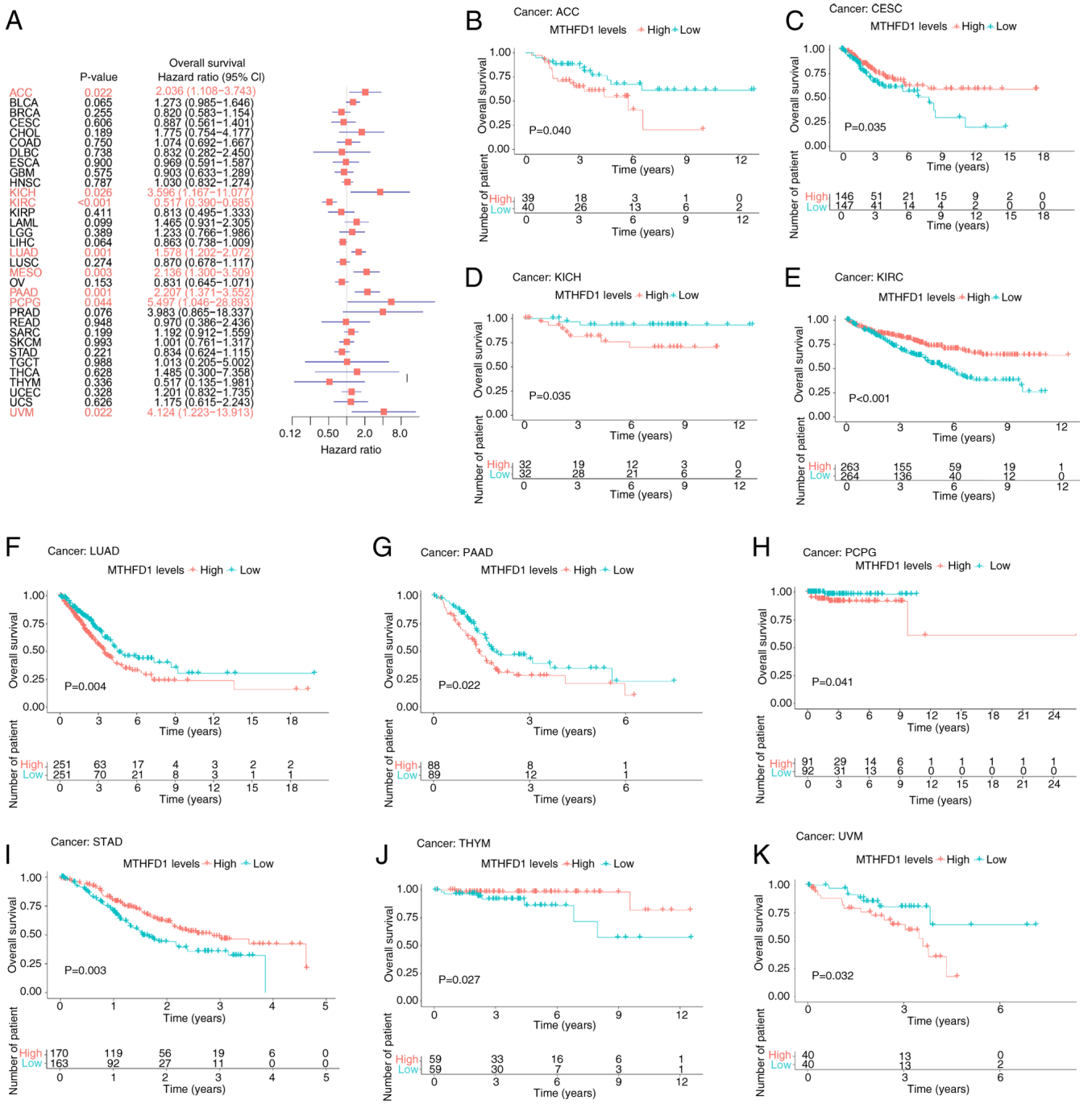

Figure 3. Prognostic value of MTHFD1 in 33 types of tumor based on OS. (A) Forest plot indicating the predictive value of MTHFD1expression for OS across different types of cancer. Kaplan-Meier survival curves demonstrating the differences in OS between patients with high or low MTHFD1 expression levels in (B) ACC, (C) CESC, (D) KICH, (E) KIRC, (F) LUAD, (G) PAAD, (H) PCPG, (I) STAD, (J) THYM and (K) UVM. MTHFD1, methylenetetrahydrofolate dehydrogenase 1; OS, overall survival; ACC, adrenal carcinoma; BLCA, bladder urothelial carcinoma; BRCA, breast invasive carcinoma; CESC, cervical squamous cell carcinoma; CHOL, cholangiocarcinoma; COAD, colon adenocarcinoma; DLBC, diffuse large B-cell lymphoma; ESCA, esophageal carcinoma; GBM, glioblastoma multiforme; HNSC, head and neck squamous cell carcinoma; KIRC, kidney renal clear cell carcinoma; KIRP, kidney renal papillary cell carcinoma; LGG, low-grade glioma; LIHC, liver hepatocellular carcinoma; LUAD, lung adenocarcinoma; LUSC, lung squamous cell carcinoma; OV, ovarian serous cystadenocarcinoma; PAAD, pancreatic adenocarcinoma; PCPG, pheochromocytoma and paraganglioma; PRAD, prostate adenocarcinoma; READ, rectum adenocarcinoma; SARC, sarcoma; SKCM, skin cutaneous melanoma; STAD, stomach adenocarcinoma; TGCT, testicular germ cell tumor; THCA, thyroid carcinoma; THYM, thymoma; UCEC, uterine corpus endometrial carcinoma; UVM, uveal melanoma.

next assessed in the present study. The results revealed a correlation between MTHFD1 expression levels and TMB in 17 types of tumor, including ACC, uterine carcinosarcoma, UCEC and THYM (Fig. 7A). Specifically, a positive correlation was observed in ACC, uterine carcinosarcoma, UCEC and other tumors, while a negative correlation was found in THYM. However, the TIDE algorithm showed no correlation in only four types of tumor, namely MESO, LIHC, DLBC and CHOL (Fig. 7B). The TIDE algorithm was used to evaluate the tumor immune dysfunction and exclusion, and all of these tumors showed a negative correlation between MTHFD1 expression levels and TIDE scores. In 2017, the

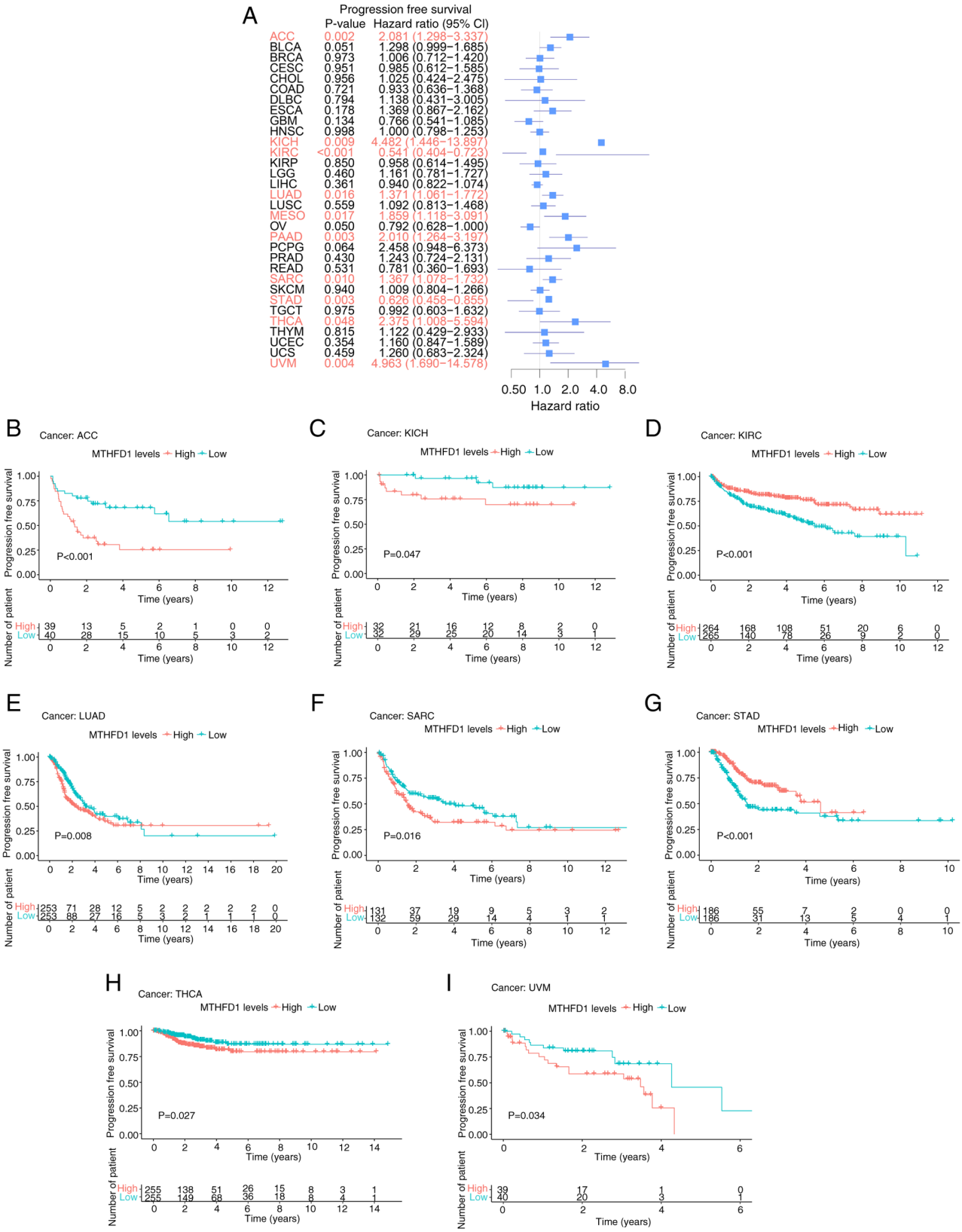

Figure 4. Prognostic value of MTHFD1 in 33 types of tumor based on PFS. (A) Forest plot indicating the predictive value of MTHFD1 for PFS across different types of cancer. Kaplan-Meier survival curves demonstrating the differences in PFS between patients with high or low MTHFD1 expression levels in (B) ACC, (C) KICH, (D) KIRC, (E) LUAD, (F) SARC, (G) STAD, (H) THCA and (I) UVM. PFS, progression-free survival; MTHFD1, methylenetetrahydrofolate dehydrogenase 1; ACC, adrenal carcinoma; BLCA, bladder urothelial carcinoma; BRCA, breast invasive carcinoma; CESC, cervical squamous cell carcinoma; CHOL, cholangiocarcinoma; COAD, colon adenocarcinoma; DLBC, diffuse large B-cell lymphoma; ESCA, esophageal carcinoma; GBM, glioblastoma multiforme; HNSC, head and neck squamous cell carcinoma; KIRC, kidney renal clear cell carcinoma; KIRP, kidney renal papillary cell carcinoma; LGG, low-grade glioma; LIHC, liver hepatocellular carcinoma; LUAD, lung adenocarcinoma; LUSC, lung squamous cell carcinoma; OV, ovarian serous cystadenocarcinoma; PAAD, pancreatic adenocarcinoma; PCPG, pheochromocytoma and paraganglioma; PRAD, prostate adenocarcinoma; READ, rectum adenocarcinoma; SARC, sarcoma; SKCM, skin cutaneous melanoma; STAD, stomach adenocarcinoma; TGCT, testicular germ cell tumor; THCA, thyroid carcinoma; THYM, thymoma; UCEC, uterine corpus endometrial carcinoma; UVM, uveal melanoma.

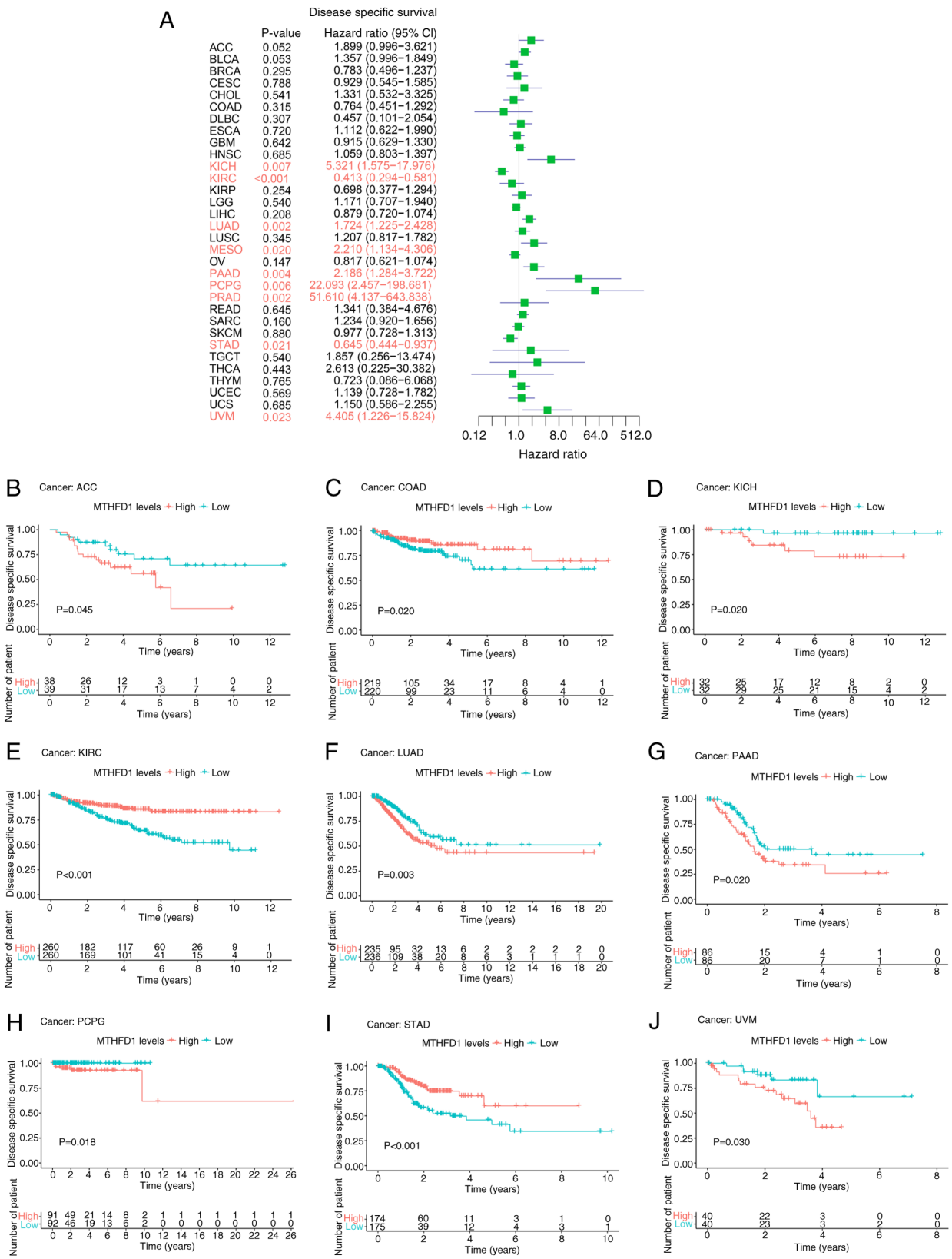

Figure 5. Prognostic value of MTHFD1 in 33 types of tumor based on DSS. (A) Forest plot showing the predictive value of MTHFD1 for DSS across different types of cancer. Kaplan-Meier survival curves demonstrating the differences in DSS between patients with high or low MTHFD1 expression levels in (B) ACC, (C) COAD, (D) KICH, (E) KIRC, (F) LUAD, (G) PAAD, (H) PCPG, (I) STAD and (J) UVM. MTHFD1, methylenetetrahydrofolate dehydrogenase 1; DSS, disease-specific survival; ACC, adrenal carcinoma; BLCA, bladder urothelial carcinoma; BRCA, breast invasive carcinoma; CESC, cervical squamous cell carcinoma; CHOL, cholangiocarcinoma; COAD, colon adenocarcinoma; DLBC, diffuse large B-cell lymphoma; ESCA, esophageal carcinoma; GBM, glioblastoma multiforme; HNSC, head and neck squamous cell carcinoma; KIRC, kidney renal clear cell carcinoma; KIRP, kidney renal papillary cell carcinoma; LGG, low-grade glioma; LIHC, liver hepatocellular carcinoma; LUAD, lung adenocarcinoma; LUSC, lung squamous cell carcinoma; OV, ovarian serous cystadenocarcinoma; PAAD, pancreatic adenocarcinoma; PCPG, pheochromocytoma and paraganglioma; PRAD, prostate adenocarcinoma; READ, rectum adenocarcinoma; SARC, sarcoma; SKCM, skin cutaneous melanoma; STAD, stomach adenocarcinoma; TGCT, testicular germ cell tumor; THCA, thyroid carcinoma; THYM, thymoma; UCEC, uterine corpus endometrial carcinoma; UVM, uveal melanoma.

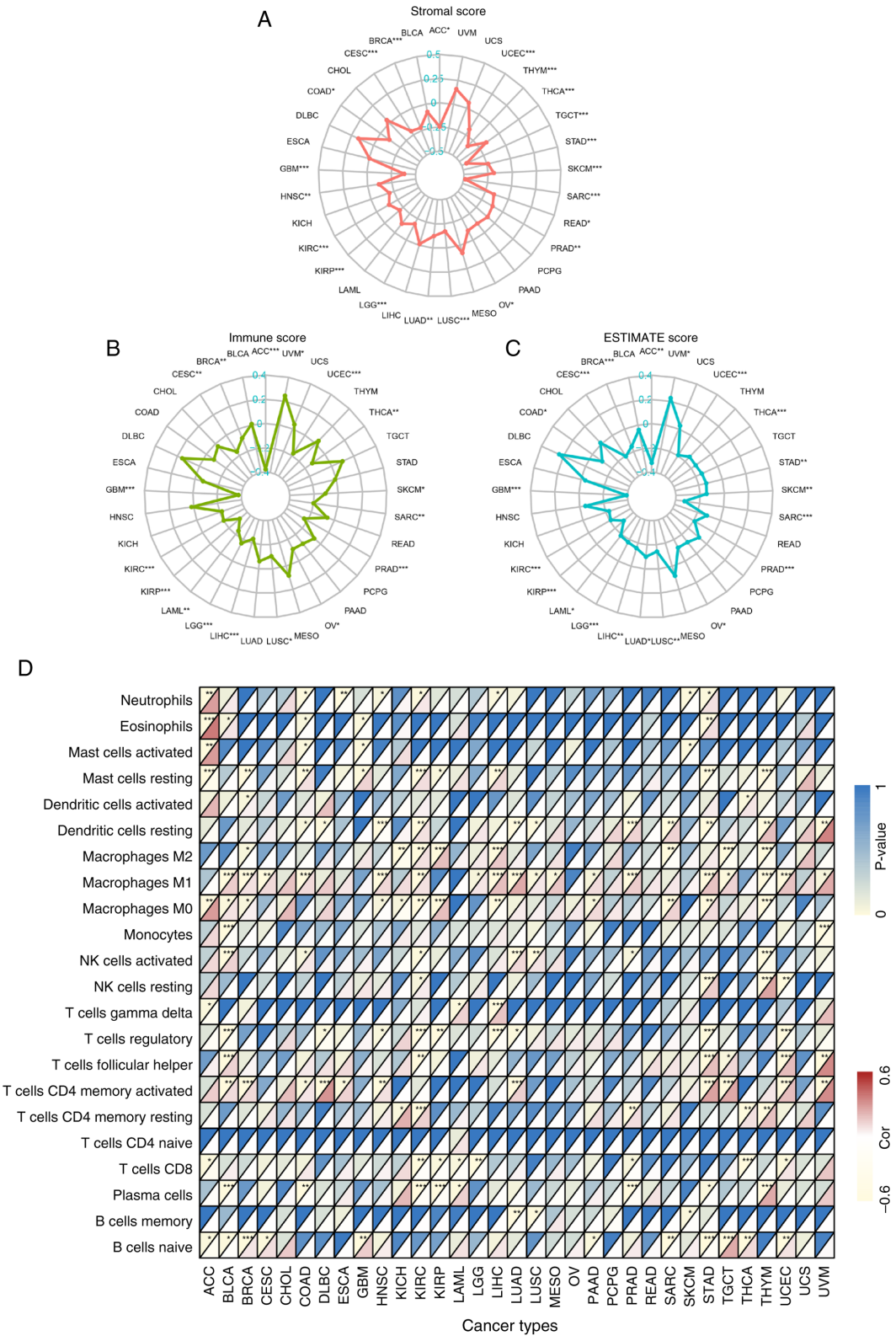

Figure 6. Correlation between the MTHFD1 expression level and the tumor microenvironment in 33 types of tumor. Radar plots demonstrating the correlation between MTHFD1 expression levels and (A) stromal, (B) immune and (C) ESTIMATE scores in different types of cancer. (D) Heatmap indicating the correlation between MTHFD1 expression levels and the abundance of 22 immune cell infiltrates in different types of cancer. In each grid, the lower triangle represents the correlation coefficient, where red indicates positive correlation and yellow indicates negative correlation. The upper triangle represents the corresponding P-value, with deeper blue indicating a smaller P-value (greater statistical significance). *P<0.05, **P<0.01 and ***P<0.001. MTHFD1, methylenetetrahydrofolate dehydrogenase 1; ACC, adrenal carcinoma; BLCA, bladder urothelial carcinoma; BRCA, breast invasive carcinoma; CESC, cervical squamous cell carcinoma; CHOL, cholangiocarcinoma; COAD, colon adenocarcinoma; DLBC, diffuse large B-cell lymphoma; ESCA, esophageal carcinoma; GBM, glioblastoma multiforme; HNSC, head and neck squamous cell carcinoma; KIRC, kidney renal clear cell carcinoma; KIRP, kidney renal papillary cell carcinoma; LGG, low-grade glioma; LIHC, liver hepatocellular carcinoma; LUAD, lung adenocarcinoma; LUSC, lung squamous cell carcinoma; OV, ovarian serous cystadenocarcinoma; PAAD, pancreatic adenocarcinoma; PCPG, pheochromocytoma and paraganglioma; PRAD, prostate adenocarcinoma; READ, rectum adenocarcinoma; SARC, sarcoma; SKCM, skin cutaneous melanoma; STAD, stomach adenocarcinoma; TGCT, testicular germ cell tumor; THCA, thyroid carcinoma; THYM, thymoma; UCEC, uterine corpus endometrial carcinoma; UVM, uveal melanoma.

FDA first approved the use of the programmed cell death protein 1 (PDCD1) inhibitor pembrolizumab (also known as Keytruda) for treating patients with solid tumors with high MSI or mismatch repair deficiency (40). Therefore, the association between MTHFD1 and MSI was also assessed in the present study. This revealed an association in nine types of tumors (Fig. 7C). Positive correlations were observed in UVM, UCEC, STAD, SARC and COAD, while negative correlations were found in THCA, HNSC, DLBC and BRCA. Furthermore, analysis of the IMvigor210 dataset revealed an increased expression of MTHFD1 in patients that responded to immune checkpoint inhibitors (ICBs) compared with those that did not respond (Fig. 7D). Considering the therapeutic potential of ICB, the correlations between MTHFD1 expression and the different ICB-related gene expression levels were further investigated using data from TCGA. There was a negative correlation between MTHFD1 expression levels and various genes, including PDCD1 in KIRC, KIRP, LIHC, THCA and THYM, CD274 in MESO, CTLA-4 in CESC, GBM, LGG, LIHC and PRAD, and TIGIT in KIRC, LGG and LIHC. By contrast, a positive correlation between MTHFD1 expression levels and PDCD1 was observed in BLCA, HNSC, LUAD and UVM, as well as with CD274 in KIRC, CTLA-4 in BLCA, and TIGIT in BLCA and UVM (Fig. 7E). In summary, these results highlighted the potential of MTHFD1 as a predictive biomarker for the response to immunotherapy in a number of tumor types.

MTHFD1 exhibits distinct roles in LUAD and KIRC. As the expression of MTHFD1 was upregulated in LUAD tumors, where high MTHFD1 expression levels were associated with reduced OS, PFS and DSS in patients with LUAD, with opposite trends revealed for KIRC tumors, the specific effects of MTHFD1 in LUAD and KIRC tumor cells was investigated further. The median expression level of MTHFD1 was calculated by ranking all of the expression level values for each type of tumor and selecting the 50th percentile. For LUAD, the median was determined to be 3.033679, whereas for KIRC it was 3.289875. These median values are indicated on the Kaplan-Meier curves in Fig. 3E and F, which were used as the cut-off thresholds to stratify patients into groups of high or low expression levels. Using these thresholds in the subsequent differential expression analysis (with an absolute log-fold change cutoff of 0.585 and a false discovery rate of 0.05, 818 and 264 DEGs were identified in LUAD and KIRC, respectively. Fig. 8 presents the results of GO and KEGG analyses of DEGs in LUAD and KIRC. In LUAD (Fig. 8A), the top enriched biological processes included 'organelle fission', 'nuclear division' and 'microtubule-based movement'. Cellular components enriched in LUAD were 'microtubule' and 'cytoplasmic region', while molecular functions included 'cytoskeletal motor activity'. KEGG pathway analysis in LUAD revealed significant enrichment in 'cAMP signaling pathway', 'neuroactive ligand-receptor interaction' and 'motor proteins'. In KIRC (Fig. 8B), the top biological processes enriched were 'acute-phase response', 'acute inflammatory response' and 'icosanoid transport'. The cellular components enriched in KIRC included 'ion channel complex' and 'blood microparticle', while molecular functions included 'gated channel activtity' and 'serine-type endopeptidase activity'. KEGG analysis in KIRC revealed significant pathways, such as 'nicotine addiction', 'neuroactive ligand-receptor interaction' and 'complement and coagulation cascades'. These results highlight the involvement of immune-related pathways and metabolic processes in tumor progression across both cancer types. Furthermore, subsequent univariate and multivariant Cox analysis (the latter adjusted for age, sex and stage) revealed that MTHFD1 expression level was an independent risk factor for prognosis in LUAD (Fig. 8C and D) and an independent protective factor for prognosis in KIRC (Fig. 8E and F). These findings suggested that MTHFD1 may have differential roles in different types of tumors.

Furthermore, *in vitro* experiments demonstrated that knocking down the expression of MTHFD1 in a LUAD cell line significantly inhibited the proliferation and migration of cells (Fig. 9A-C). In addition, the overexpression of MTHFD1 in a KIRC cell line significantly reduced the proliferation and migration of cells (Fig. 9D-F). Taken together, these results indicated that MTHFD1 may have an oncogenic role in LUAD, as well as a tumor suppressive role in KIRC.

Discussion

The present study investigated the expression levels of the amino acid metabolism-related gene MTHFD1 across 33 types of cancer. The impact of MTHFD1 on the prognosis and immune status, particularly in predicting immunotherapy efficacy, was also assessed. The results of the present study indicated that MTHFD1 had a role in various types of cancer, including LUAD and KIRC. Data from TCGA indicated that MTHFD1 had differential expression levels in 18 types of cancer compared with those in their normal tissue counterparts. Among these, 13 types of cancer indicated upregulated MTHFD1 expression levels in tumor tissues, including BLCA, CESC, COAD, ESCA, GBM, HNSC, LUAD, LUSC, PRAD, READ, STAD and UCEC. By contrast, decreased MTHFD1 expression levels were indicated in BRCA, KICH, KIRC, LIHC and PCPG. Additionally, data from the CPTAC also indicated these trends in the expression of MTHFD1 in BRCA, COAD, KIRC, UCEC, LUAD, GBM and LIHC. This suggested that MTHFD1 may have mechanistic differences in various tumors.

Further analysis of prognostic data revealed that high MTHFD1 expression levels were associated with a reduced OS in ACC, KICH, LUAD, PAAD, PCPG and UVM. However, an opposite trend was demonstrated in KIRC. PFS analysis indicated that patients with low MTHFD1 expression levels had a longer PFS in ACC, KICH, LUAD, SARC, THCA and UVM compared with those with high MTHFD1 expression levels. However, the opposite was demonstrated in KIRC and STAD. DSS trends mostly mirrored those of OS, except in ACC, where the survival curve showed significance, but the association was not statistically significant in the univariate Cox regression analysis and was therefore excluded. By contrast, the association was statistically significant in STAD.

Overall, the data obtained from a number of databases suggested that the expression of MTHFD1 was downregulated in KIRC compared with that in normal tissues, with high MTHFD1 expression levels associated with a favorable prognosis, which may indicate a tumor suppressive role. However, in

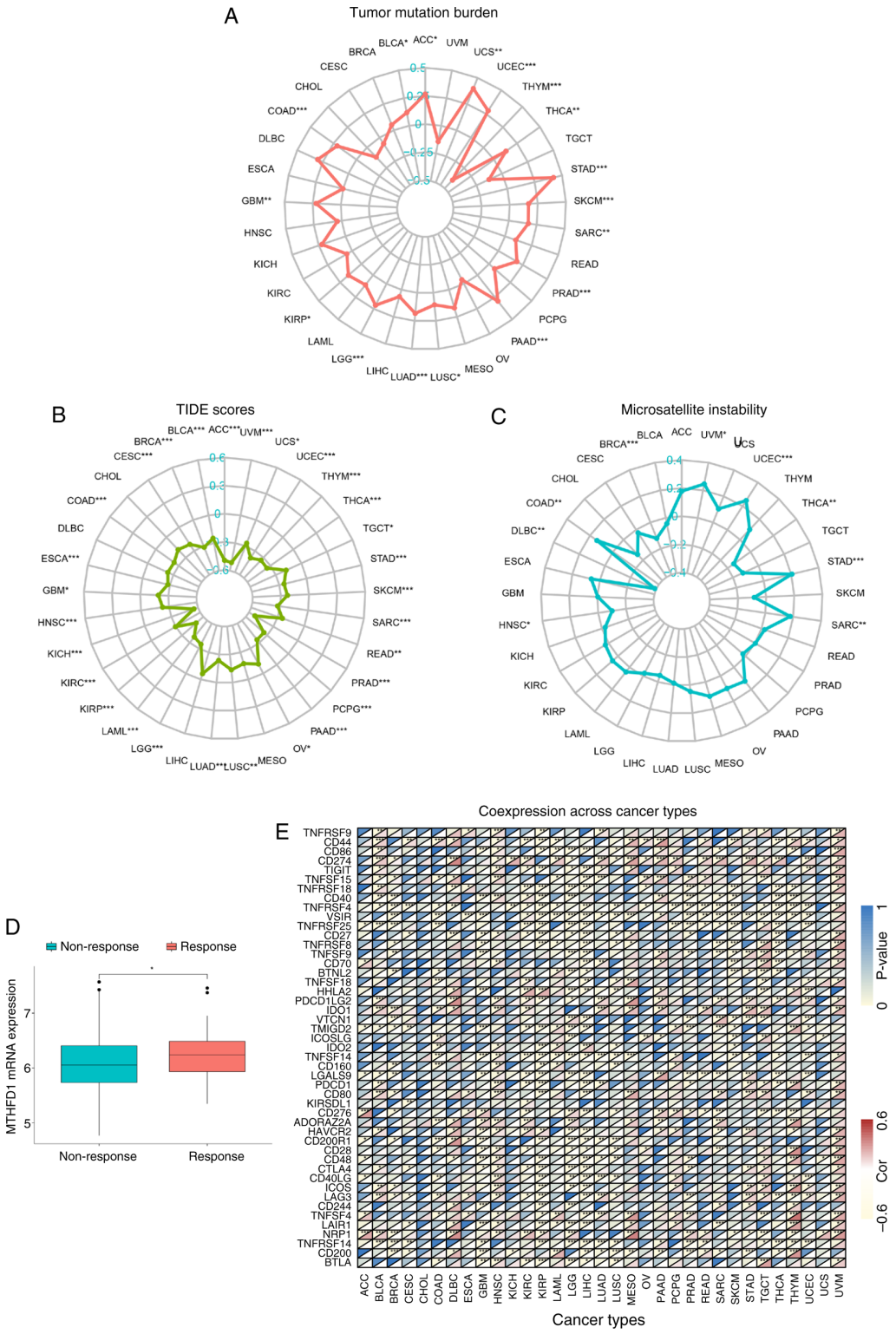

Figure 7. Predictive potential of MTHFD1 in immunotherapy across 33 types of tumor. Radar plots demonstrating the correlation between MTHFD1 and (A) tumor mutational burden, (B) TIDE scores and (C) microsatellite instability in different types of cancer. (D) Boxplot of the IMvigor210 dataset showing the differences in MTHFD1 expression levels between patients who responded to atezolizumab (PD-L1 inhibitor) treatment and those who did not. (E) Heatmap indicating the correlation between the expression of MTHFD1 and 48 immune checkpoint blockade-related genes in different types of cancer. In each grid, the lower triangle represents the correlation coefficient, where red indicates positive correlation and yellow indicates negative correlation. The upper triangle represents the corresponding P-value, with deeper blue indicating a smaller P-value (greater statistical significance). *P<0.05, **P<0.01 and ***P<0.001. MTHFD1, methylenetetrahydrofolate dehydrogenase 1; TIDE, tumor immune dysfunction, and exclusion; ACC, adrenal carcinoma; BLCA, bladder urothelial carcinoma; BRCA, breast invasive carcinoma; CESC, cervical squamous cell carcinoma; CHOL, cholangiocarcinoma; COAD, colon adenocarcinoma; DLBC, diffuse large B-cell lymphoma; ESCA, esophageal carcinoma; GBM, glioblastoma multiforme; HNSC, head and neck squamous cell carcinoma; KIRC, kidney renal clear cell carcinoma; KIRP, kidney renal papillary cell carcinoma; LGG, low-grade glioma; LIHC, liver hepatocellular carcinoma; LUAD, lung adenocarcinoma; LUSC, lung squamous cell carcinoma; OV, ovarian serous cystadenocarcinoma; PAAD, pancreatic adenocarcinoma; PCPG, pheochromocytoma and paraganglioma; PRAD, prostate adenocarcinoma; READ, rectum adenocarcinoma; SARC, sarcoma; SKCM, skin cutaneous melanoma; STAD, stomach adenocarcinoma; TGCT, testicular germ cell tumor; THCA, thyroid carcinoma; THYM, thymoma; UCEC, uterine corpus endometrial carcinoma; UVM, uveal melanoma.

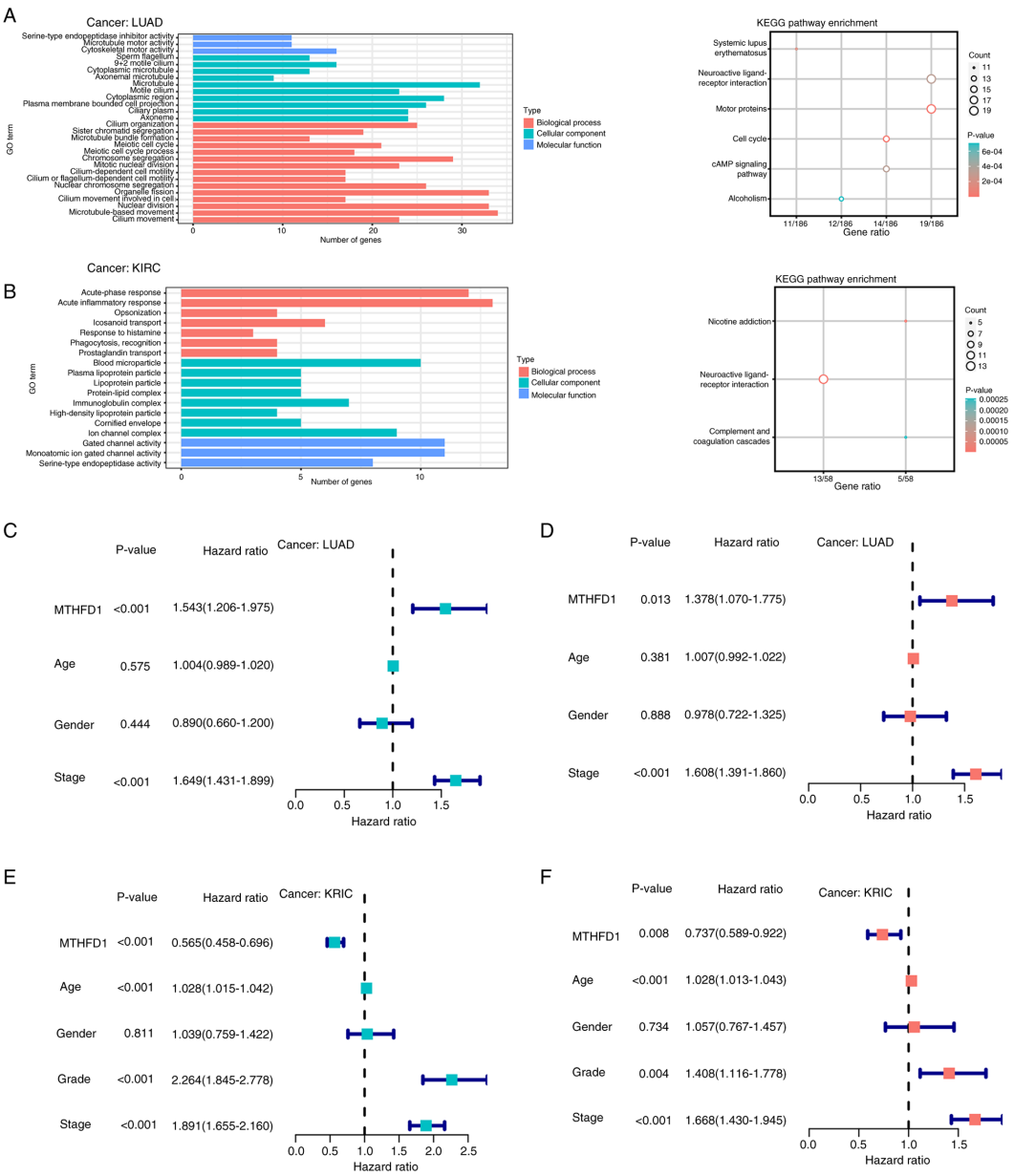

Figure 8. Role of MTHFD1 in LUAD and KIRC. GO and KEGG analysis of the biological functions of differentially expressed genes between the high and low MTHFD1 expression level groups in (A) LUAD and (B) KIRC. Forest plots showing (C) univariate and (D) multivariate Cox analyses of MTHFD1 in LUAD. Forest plots showing the (E) univariate and (F) multivariate Cox analyses of MTHFD1 in KIRC. MTHFD1, methylenetetrahydrofolate dehydrogenase 1; GO, Gene Ontology; KEGG, Kyoto Encyclopedia of Genes and Genomes; LUAD, lung adenocarcinoma; KIRC, kidney renal clear cell carcinoma.

LUAD, MTHFD1 may serve as an oncogene, since its expression levels and prognostic trends were the opposite of those for KIRC. These findings align with previous studies that indicate the variable roles of the same gene/protein across different types of cancer. A previous study by Li *et al* (41) revealed that the microtubule associated monooxygenase, calponin and LIM domain-containing gene is an oncogene in KIRC, but a tumor suppressor in PAAD and LUAD. Another study by Cao *et al* (42) reported that the lysine N-methyltransferase 2C gene is a protective factor in KIRC and ovarian serous cystadenocarcinoma, but a risk factor in LUSC and UVM. There heterogeneity of tumors and the microenvironmental differences may contribute to the diverse roles that a protein has in different types of cancer (43). Furthermore, results of the ssGSEA algorithm indicated that MTHFD1 activity was increased in 21 tumor tissues compared with that in the normal tissue counterparts, suggesting that MTHFD1 may play a dual role in cancer, by promoting tumor growth and progression by modulating amino acid metabolism in some cancers, while potentially inhibiting tumor development in others.

To further investigate the differential roles of MTHFD1 in various types of tumors and its influence on immune cells, an in-depth analysis of its association with immune cell infiltration was next performed. The results, as indicated using the ESTIMATE algorithm, revealed a significant correlation between MTHFD1 expression levels and immune cell infiltration across 17 types of tumors, albeit with notable differences among different types of cancer. In UVM, MTHFD1 expression levels were positively correlated with immune scores, suggesting an immunoactive environment characterized by

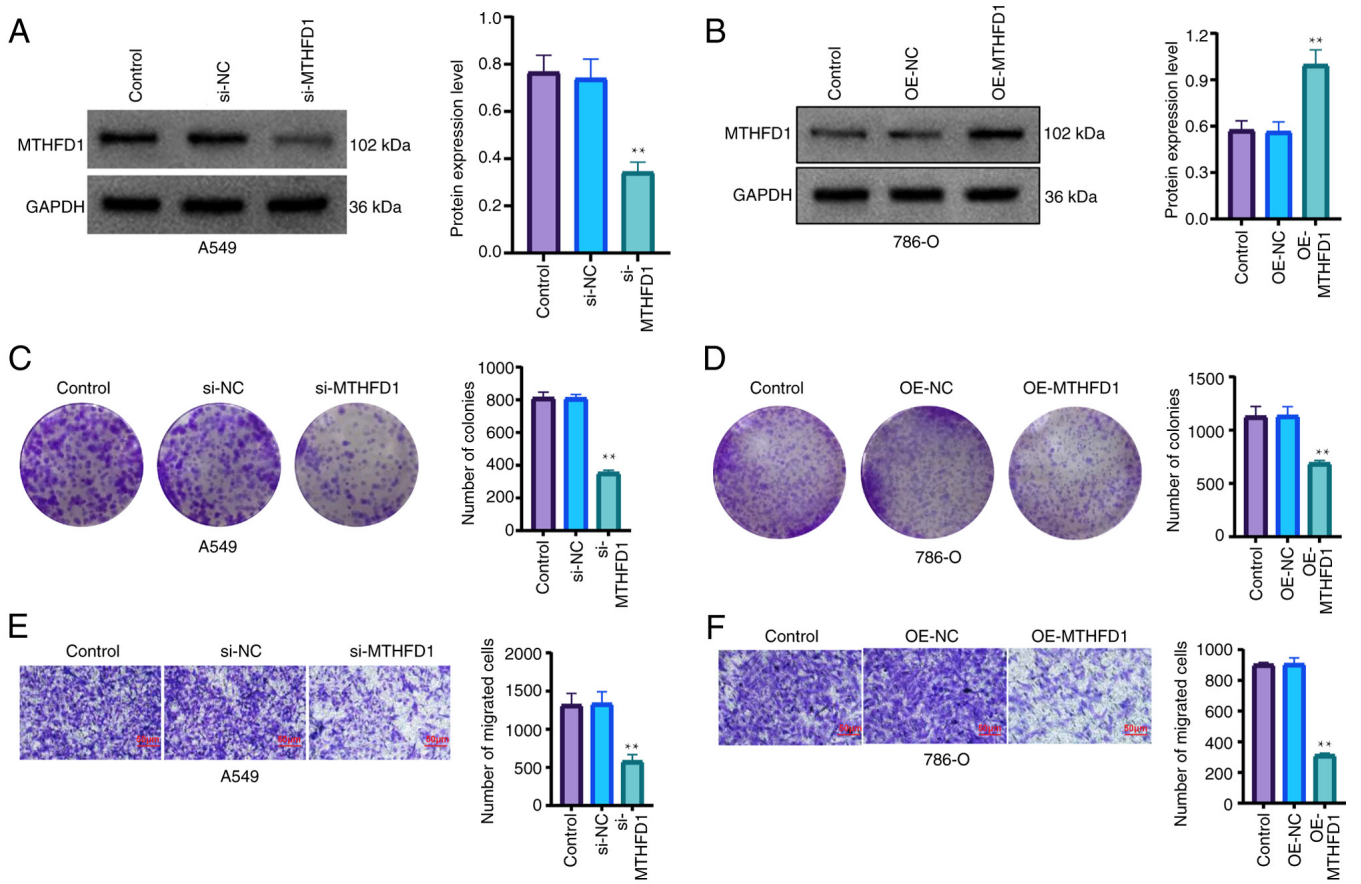

Figure 9. Role of MTHFD1 in LUAD and KIRC cell lines. Western blot analysis showing the expression of MTHFD1 after transfection with (A) si-MTHFD1 in LUAD or (B) OE-MTHFD1 plasmids in KICH cell lines. Colony formation assay demonstrating the proliferation of cells after transfection with (C) si-MTHFD1 in LUAD or (D) OE-MTHFD1 plasmids in KICH cell lines. Transwell migration assay showing the migration of cells after transfection with (E) si-MTHFD1 in LUAD or (F) OE-MTHFD1 plasmids in KICH cell lines. **P<0.01. MTHFD1, methylenetetrahydrofolate dehydrogenase 1; LUAD, lung adenocarcinoma; KIRC, kidney renal clear cell carcinoma; si; small interfering; OE, overexpression; NC, negative control.

enhanced immune cell infiltration, particularly CD4 T cells and dendritic cells, which may promote antitumor immunity. By contrast, in ACC, MTHFD1 expression levels were negatively correlated with immune scores. COAD, in which the MTHFD1 expression levels were increased compared with those in normal tissues, is positively correlated with pro-tumor immune cells, such as resting mast cells. These cells secrete IL-10, TGF-β and VEGF, which suppress immune responses and promote angiogenesis (44-48). By contrast, in other types of cancer, such as LIHC, in which the MTHFD1 expression levels were decreased compared with those in normal tissues, MTHFD1 was negatively correlated with pro-tumor immune cells, such as Tregs, but was positively correlated with antitumor immune cells, including M1 macrophages. M1 macrophages secrete TNF-α and IL-12, which eliminate tumor cells and activate other immune cells, including $CD8^+$ T cells and natural killer cells (49). By contrast, Tregs can weaken the antitumor effect of the immune system by inhibiting the activity of cytotoxic T cells and natural killer cells (50). In KIRC, MTHFD1 expression was correlated with 13 types of immune cell types, with 6 types negatively correlated (e.g., plasma cells) and 7 types positively correlated (e.g., neutrophils), suggesting robust immune cell infiltration and a potential tumor-suppressing role. However, in LUAD, MTHFD1 expression was correlated with only six types of immune cells, with three types positively correlated (e.g., M1 macrophages) and three types negatively correlated (e.g., memory B cells). These results indicate that MTHFD1 may influence tumor progression by modulating immune cell activity. In certain types of cancer, such as KIRC, LUAD and UVM, MTHFD1 may enhance antitumor immune cell function, promoting an 'activated' immune microenvironment. By contrast, in other types of cancer, it may promote pro-tumor immune cell functions, resulting in an immunosuppressive state. However, the complexity of cancer should be acknowledged, as genes may impact tumor progression through various mechanisms beyond immune cells, such as the regulation of the cell cycle and proliferation by transcription factors such as FOXM1, epigenetic modifications leading to gene silencing, remodeling of the extracellular matrix in the tumor microenvironment, and metabolic reprogramming to support rapid tumor growth and invasion (51-53). Furthermore, GO and KEGG enrichment analyses suggested that in LUAD, MTHFD1 may promote tumor progression by enhancing biological processes such as 'nuclear division', 'organelle fission' and 'microtubule-based movement'. Cellular components such as the 'microtubule' and 'cytoplasmic region' were enriched, while molecular functions related to 'cytoskeletal motor activity' were identified. KEGG pathway analysis revealed significant involvement of pathways such as the

'cAMP signaling pathway', which could support cell survival, and 'neuroactive ligand-receptor interaction', potentially contributing to tumorigenesis. These results highlight the role of MTHFD1 in driving key cellular functions and metabolic pathways that promote LUAD progression. MTHFD1 has been previously documented to enhance tumor cell migration and invasion in colorectal cancer by modulating cytoskeletal and adhesion molecules, such as by regulating actin filament rearrangement and integrin expression, thereby increasing the risk of metastasis (54). In addition, its role in the cAMP signaling pathway may also facilitate the proliferation of cancer cells, particularly in bladder cancer, where it is involved in the induction of 7-dehydrocholesterol reductase, stimulating cholesterol synthesis and activating cAMP signaling to promote metastasis (55). These mechanisms highlight the potential of MTHFD1 as an oncogenic factor and a therapeutic target in LUAD. By contrast, in KIRC, MTHFD1 may exert tumor suppressing effects by regulating acute inflammatory responses, complement and coagulation cascades and the functions of cell membrane channels. These mechanisms may enhance antitumor immunity and facilitate the clearance of cancer cells, as supported by studies on inflammation, immune regulation, and coagulation pathways (56-59). The multifaceted role of MTHFD1 in KIRC as a tumor suppressor highlighted it as a potential therapeutic target. Potential strategies to target MTHFD1 in KIRC include using gene silencing techniques such as RNA interference or CRISPR-Cas9 to reduce MTHFD1 expression, developing small molecule inhibitors to block its enzymatic activity, or employing gene therapy approaches to either restore its function or inhibit its overexpression in tumor cells. Preliminary *in vitro* experiments further indicated the divergent roles of MTHFD1 in LUAD and KIRC, which highlighted its potential in different types of cancer.

Given the role of immunotherapy in the treatment of cancer (60), in the present study, the efficacy of MTHFD1 in immunotherapy across 33 different tumor types was analyzed using the TIDE algorithm. However, it should be noted that MTHFD1 has not yet been FDA-approved as an immunotherapy target for all these cancer types, and its efficacy in immunotherapy remains under investigation. The results indicated that a high expression of MTHFD1 was significantly associated with poorer responses to immunotherapy, as indicated by negative correlations with TIDE scores, suggesting that higher MTHFD1 expression is linked to immune escape and resistance to treatment in most cancers studied. However, no significant correlation was observed in LIHC, DLBC, MESO and CHOL. Further analysis from the IMvigor database also suggested a role of MTHFD1 in immunotherapy. TIDE scores and IMvigor data are used to reflect the efficacy response of PDCD1/PD-L1 and cytotoxic T-lymphocyte-associated protein 4 (CTLA-4) inhibitors (61,62) A previous study identified MTHFD1 as a potential therapeutic target in prostate cancer, associating its expression with poor survival outcomes and suggesting that targeting MTHFD1 could enhance immunotherapy efficacy (63). MTHFD1 is a key enzyme in the one-carbon metabolism pathway and is responsible for converting folate metabolites into active one-carbon units used for DNA synthesis, nucleic acid synthesis and methionine regeneration. These processes are important for sustaining rapid tumor cell proliferation and immune cell activation (64-66). By promoting these reactions involved in metabolite synthesis, MTHFD1 provides sufficient metabolic support for T cells, enhancing their activity within the TME, including in colorectal cancer, bladder cancer and tongue squamous cell carcinoma (67). Adequate nucleic acid supply aids in T cell proliferation, boosting their cytotoxic effects on tumor cells and increasing the sensitivity of tumor cells to PDCD1/PD-L1 and CTLA-4 inhibitors, without promoting tumor cell proliferation directly (68). Secondly, the role of MTHFD1 in amino acid metabolism notably impacts the TME (36,69). It participates in serine and glycine synthesis, which are key for cell proliferation and metabolic activities (22). By promoting these metabolic pathways, MTHFD1 may reduce the capacity of tumor cell immune evasion and in certain circumstances, such as in colorectal and bladder cancer, inhibit the production of immunosuppressive metabolites, such as adenosine (70-72). Adenosine is a immunosuppressive molecule, where a reduction in its levels can enhance the efficacy of ICBs (72). Additionally, MTHFD1 may influence the balance of immune cell subsets, particularly by reducing the proportion of Tregs, which are known immunosuppressive cells that weaken immune responses by inhibiting the function of effector T cells. MTHFD1 may regulate Treg activity through its metabolic products, such as methylenetetrahydrofolate, formylmethionine, serine and glycine (71). These metabolites can reduce immune suppression and enhance antitumor immune effects (73). Additionally, similar to other genes, such as CTLA4 and DRD1 (74,75), methylation reactions involving MTHFD1 not only regulate gene expression levels in tumor cells but also affect PD-L1 and CTLA-4 expression levels in tumor and immune cells, further improving the effectiveness of immunotherapy. The results of the present study also demonstrated that MTHFD1 had significant positive correlations with key ICB genes, such as PDCD1 in LUAD, CTLA-4 in BLCA and TIGIT in UVM. This suggested that MTHFD1 may serve as a potential biomarker for evaluating the response to immunotherapy. However, negative correlations with certain immunosuppressive checkpoints, such as PDCD1 in KIRC, CD274 in MESO, CTLA-4 in CESC and TIGIT in KIRC, implied that MTHFD1 may enhance antitumor immune responses by downregulating these inhibitory pathways. Therefore, MTHFD1 is potentially valuable in immunotherapy due to its possible modulation of metabolic pathways, influence on immune cell functions and production of a favorable TME. Future studies should focus on clinically validating these findings and further investigating the specific biological mechanisms of MTHFD1 in immunotherapy to develop novel therapeutic strategies and enhance the efficacy of immunotherapy.

To the best of our knowledge, the present study was the first to provide a comprehensive analysis of the amino acid metabolism-related gene MTHFD1. The results indicted its varied expression patterns across multiple types of cancer and highlighted its associations with patient survival, tumor progression and the immune microenvironment. The findings of the present study highlighted the role of MTHFD1 in different tumor types and indicated its potential application in precision medicine for diagnosis and treatment. Furthermore,

the present study indicated that high MTHFD1 expression levels were associated with the response of certain types of cancer to ICBs, such as drugs targeting PDCD1/PD-L1 and CTLA-4. MTHFD1 demonstrated distinct correlations with various immune checkpoint pathways, which indicated its value as a potential biomarker for immunotherapy. This evidence supports the translation of research on MTHFD1 from the laboratory into a clinically significant diagnostic and therapeutic target, paving the way for personalized treatment strategies, and improving the effectiveness and precision of immunotherapy.

Although the present study indicated the role of MTHFD1 in a pan-cancer panel, it had a number of limitations. The conclusions drawn used data from public databases and lacked primary data obtained from patients. In addition, tumor tissues are heterogeneous, where bulk data from databases, such as TCGA, may not reflect the genetic changes within tumor cells. The present study also lacked single-cell sequencing data to further investigate the molecular mechanisms involved. In addition, the present study lacked immune cell infiltration experiments using animal and clinical specimens. The *in vitro* experiments performed in the present study were limited to two types of cancer, which therefore lacked a comprehensive analysis and mechanistic investigation into other types of tumors. The present study also lacked an investigation into the specific mechanisms underlying the efficacy of immunotherapy.

In conclusion, the results of the present study indicated the potential oncogenic role of MTHFD1 in LUAD and its tumor suppressive role in KIRC *in vitro*. Furthermore, it was demonstrated that high MTHFD1 expression levels were associated with decreased immune cell infiltration in various types of cancer and may serve as a predictive marker for the response to immunotherapy. In future studies, MTHFD1 should be further investigated to enhance the experimental and clinical data, which may provide novel insights into its role in the prognosis and treatment of tumors, particularly in the context of immunotherapy.

Acknowledgements

Not applicable.

Funding

No funding was received.

Availability of data and materials

The data generated in the present study may be requested from the corresponding author.

Authors' contributions

SG and ChuP conceived the study. JY designed the study. ChaP conducted the cell experiments and collected the data. SG and ChuP wrote the manuscript. FP analyzed the data. SG and ChuP confirm the authenticity of all the raw data. All authors read and approved the final version of the manuscript.

Ethics approval and consent to participate

Not applicable.

Patient consent for publication

Not applicable.

Competing interests

The authors declare that they have no competing interests.

References

1. Sung H, Ferlay J, Siegel RL, Laversanne M, Soerjomataram I, Jemal A and Bray F: Global cancer statistics 2020: GLOBOCAN estimates of incidence and mortality worldwide for 36 cancers in 185 countries. CA Cancer J Clin 71: 209-249, 2021.
2. Zeng H, Chen W, Zheng R, Zhang S, Ji JS, Zou X, Xia C, Sun K, Yang Z, Li H, *et al*: Changing cancer survival in China during 2003-15: A pooled analysis of 17 population-based cancer registries. Lancet Glob Heal 6: e555-e567, 2018.
3. Chang JH, Wu CC, Yuan KSP, Wu ATH and Wu SY: Locoregionally recurrent head and neck squamous cell carcinoma: Incidence, survival, prognostic factors, and treatment outcomes. Oncotarget 8: 55600-55612, 2017.
4. Nors J, Iversen LH, Erichsen R, Gotschalck KA and Andersen CL: Incidence of recurrence and time to recurrence in stage I to III colorectal cancer: A nationwide Danish cohort study. JAMA Oncol 10: 54-62, 2024.
5. Liu X, Ren B, Ren J, Gu M, You L and Zhao Y: The significant role of amino acid metabolic reprogramming in cancer. Cell Commun Signal 22: 380, 2024.
6. Zhang J, Chen M, Yang Y, Liu Z, Guo W, Xiang P, Zeng Z, Wang D and Xiong W: Amino acid metabolic reprogramming in the tumor microenvironment and its implication for cancer therapy. J Cell Physiol 239: e31349, 2024.
7. Liu Y, Zhao Y, Song H, Li Y, Liu Z, Ye Z, Zhao J, Wu Y, Tang J and Yao M: Metabolic reprogramming in tumor immune microenvironment: Impact on immune cell function and therapeutic implications. Cancer Lett 597: 217076, 2024.
8. Liu Y, Zhao T, Li Z, Wang L, Yuan S and Sun L: The role of ASCT2 in cancer: A review. Eur J Pharmacol 837: 81-87, 2018.
9. Zhang Z, Liu R, Shuai Y, Huang Y, Jin R, Wang X and Luo J: ASCT2 (SLC1A5)-dependent glutamine uptake is involved in the progression of head and neck squamous cell carcinoma. Br J Cancer 122: 82-93, 2020.
10. Cormerais Y, Vučetić M, Parks SK and Pouyssegur J: Amino acid transporters are a vital focal point in the control of mTORC1 signaling and cancer. Int J Mol Sci 22: 23, 2020.
11. van Geldermalsen M, Wang Q, Nagarajah R, Marshall AD, Thoeng A, Gao D, Ritchie W, Feng Y, Bailey CG, Deng N, *et al*: ASCT2/SLC1A5 controls glutamine uptake and tumour growth in triple-negative basal-like breast cancer. Oncogene 35: 3201-3208, 2016.
12. Najumudeen AK, Ceteci F, Fey SK, Hamm G, Steven RT, Hall H, Nikula CJ, Dexter A, Murta T, Race AM, *et al*: The amino acid transporter SLC7A5 is required for efficient growth of KRAS-mutant colorectal cancer. Nat Genet 53: 16-26, 2021.
13. Ohgaki R, Hirase Y, Xu M, Okanishi H and Kanai Y: LAT1 expression in colorectal cancer cells is unresponsive to HIF-1/2α accumulation under experimental hypoxia. Sci Rep 14: 19635, 2024.
14. Hayase S, Kumamoto K, Saito K, Kofunato Y, Sato Y, Okayama H, Miyamoto K, Ohki S and Takenoshita S: L-type amino acid transporter 1 expression is upregulated and associated with cellular proliferation in colorectal cancer. Oncol Lett 14: 7410-7416, 2017.
15. Zhang Y, Xu Y, Lu W, Ghergurovich JM, Guo L, Blair IA, Rabinowitz JD and Yang X: Upregulation of antioxidant capacity and nucleotide precursor availability suffices for oncogenic transformation. Cell Metab 33: 94-109.e8, 2021.

16. Hu K, Li K, Lv J, Feng J, Chen J, Wu H, Cheng F, Jiang W, Wang J, Pei H, *et al*: Suppression of the SLC7A11/glutathione axis causes synthetic lethality in KRAS-mutant lung adenocarcinoma. J Clin Invest 130: 1752-1766, 2020.
17. Yang C, Chen J, Yu Z, Luo J, Li X, Zhou B and Jiang N: Mining of RNA methylation-related genes and elucidation of their molecular biology in gallbladder carcinoma. Front Oncol 11: 621806, 2021.
18. Chen K, Wu S, Ye S, Huang H, Zhou Y, Zhou H, Wu S, Mao Y, Shangguan F, Lan L and Chen B: Dimethyl fumarate induces metabolic crisie to suppress pancreatic carcinoma. Front Pharmacol 12: 617714, 2021.
19. Tarragó-Celada J, Foguet C, Tarrado-Castellarnau M, Marin S, Hernández-Alias X, Perarnau J, Morrish F, Hockenbery D, Gomis RR, Ruppin E, *et al*: Cysteine and folate metabolism are targetable vulnerabilities of metastatic colorectal cancer. Cancers (Basel) 13: 425, 2021.
20. Ding K, Jiang J, Chen L and Xu X: Methylenetetrahydrofolate dehydrogenase 1 silencing expedites the apoptosis of non-small cell lung cancer cells via modulating DNA methylation. Med Sci Monit 24: 7499-7507, 2018.
21. Zheng Y, Zhu L, Qin ZY, Guo Y, Wang S, Xue M, Shen KY, Hu BY, Wang XF, Wang CQ, *et al*: Modulation of cellular metabolism by protein crotonylation regulates pancreatic cancer progression. Cell Rep 42: 112666, 2023.
22. Pan S, Fan M, Liu Z, Li X and Wang H: Serine, glycine and one-carbon metabolism in cancer (review). Int J Oncol 58: 158-170, 2021.
23. Fan J, Ye J, Kamphorst JJ, Shlomi T, Thompson CB and Rabinowitz JD: Quantitative flux analysis reveals folate-dependent NADPH production. Nature 510: 298-302, 2014.
24. Lu SC and Mato JM: S-adenosylmethionine in liver health, injury, and cancer. Physiol Rev 92: 1515-1542, 2012.
25. MacFarlane AJ, Perry CA, Girnary HH, Gao D, Allen RH, Stabler SP, Shane B and Stover PJ: Mthfd1 is an essential gene in mice and alters biomarkers of impaired one-carbon metabolism. J Biol Chem 284: 1533-1539, 2009.
26. Lunt SY and Vander Heiden MG: Aerobic glycolysis: Meeting the metabolic requirements of cell proliferation. Annu Rev Cell Dev Biol 27: 441-464, 2011.
27. Feitelson MA, Arzumanyan A, Kulathinal RJ, Blain SW, Holcombe RF, Mahajna J, Marino M, Martinez-Chantar ML, Nawroth R, Sanchez-Garcia I, *et al*: Sustained proliferation in cancer: Mechanisms and novel therapeutic targets. Semin Cancer Biol 35 (Suppl 1): S25-S54, 2015.
28. Mullen NJ and Singh PK: Nucleotide metabolism: A pan-cancer metabolic dependency. Nat Rev Cancer 23: 275-294, 2023.
29. Dong Y, Zhao H, Li H, Li X and Yang S: DNA methylation as an early diagnostic marker of cancer (review). Biomed Rep 2: 326-330, 2014.
30. Dutta H and Jain N: Post-translational modifications and their implications in cancer. Front Oncol 13: 1240115, 2023.
31. Becht E, Giraldo NA, Lacroix L, Buttard B, Elarouci N, Petitprez F, Selves J, Laurent-Puig P, Sautès-Fridman C, Fridman WH and de Reyniès A: Estimating the population abundance of tissue-infiltrating immune and stromal cell populations using gene expression. Genome Biol 17: 218, 2016.
32. Newman AM, Liu CL, Green MR, Gentles AJ, Feng W, Xu Y, Hoang CD, Diehn M and Alizadeh AA: Robust enumeration of cell subsets from tissue expression profiles. Nat Methods 12: 453-457, 2015.
33. Hänzelmann S, Castelo R and Guinney J: GSVA: Gene set variation analysis for microarray and RNA-seq data. BMC Bioinformatics 14: 7, 2013.
34. Ritchie ME, Phipson B, Wu D, Hu Y, Law CW, Shi W and Smyth GK: limma powers differential expression analyses for RNA-sequencing and microarray studies. Nucleic Acids Res 43: e47, 2015.
35. Wu T, Hu E, Xu S, Chen M, Guo P, Dai Z, Feng T, Zhou L, Tang W, Zhan L, *et al*: clusterProfiler 4.0: A universal enrichment tool for interpreting omics data. Innovation (Camb) 2: 100141, 2021.
36. Wang W, Gu W, Tang H, Mai Z, Xiao H, Zhao J and Han J: The emerging role of MTHFD family genes in regulating the tumor immunity of oral squamous cell carcinoma. J Oncol 2022: 4867730, 2022.
37. Cao J, Ding X, Ji J, Zhang L and Luo C: Efficacy and safety of immune checkpoint inhibitors rechallenge in advanced solid tumors: A systematic review and meta-analysis. Front Oncol 14: 1475502, 2024.
38. Ma W, Xue R, Zhu Z, Farrukh H, Song W, Li T, Zheng L and Pan CX: Increasing cure rates of solid tumors by immune checkpoint inhibitors. Exp Hematol Oncol 12: 10, 2023.
39. Anagnostou V, Bardelli A, Chan TA and Turajlic S: The status of tumor mutational burden and immunotherapy. Nat Cancer 3: 652-656, 2022.
40. Hong YD, Enewold L, Halpern MT, Zeruto C and Mariotto AB: Use of pembrolizumab among older adults with cancer in the United States, before and after FDA approval of its tumor-agnostic indication. Pharmacoepidemiol Drug Saf 33: e5745, 2024.
41. Li C, Xiao Y, Kong J, Lai C, Chen Z, Li Z and Xie W: Elucidating the role of MICAL1 in pan-cancer using integrated bioinformatics and experimental approaches. Cell Adh Migr 18: 1-17, 2024.
42. Cao W, Xie Y, Cai L, Wang M, Chen Z, Wang Z, Xv J, Wang Y, Li R, Liu X and Wang W: Pan-cancer analysis on the role of KMT2C expression in tumor progression and immunotherapy. Oncol Lett 28: 444, 2024.
43. Zhang A, Miao K, Sun H and Deng CX: Tumor heterogeneity reshapes the tumor microenvironment to influence drug resistance. Int J Biol Sci 18: 3019-3033, 2022.
44. Tzorakoleftheraki SE and Koletsa T: The complex role of mast cells in head and neck squamous cell carcinoma: A systematic review. Medicina (Kaunas) 60: 1173, 2024.
45. Derakhshani A, Vahidian F, Alihasanzadeh M, Mokhtarzadeh A, Lotfi Nezhad P and Baradaran B: Mast cells: A double-edged sword in cancer. Immunol Lett 209: 28-35, 2019.
46. Mocellin S, Marincola FM and Young HA: Interleukin-10 and the immune response against cancer: A counterpoint. J Leukoc Biol 78: 1043-1051, 2005.
47. Ribatti D, Ennas MG, Vacca A, Ferreli F, Nico B, Orru S and Sirigu P: Tumor vascularity and tryptase-positive mast cells correlate with a poor prognosis in melanoma. Eur J Clin Invest 33: 420-425, 2003.
48. Watabe T, Takahashi K, Pietras K and Yoshimatsu Y: Roles of TGF-β signals in tumor microenvironment via regulation of the formation and plasticity of vascular system. Semin Cancer Biol 92: 130-138, 2023.
49. Chiba Y, Mizoguchi I, Furusawa J, Hasegawa H, Ohashi M, Xu M, Owaki T and Yoshimoto T: Interleukin-27 exerts its anti-tumor effects by promoting differentiation of hematopoietic stem cells to M1 macrophages. Cancer Res 78: 182-194, 2018.
50. Togashi Y, Shitara K and Nishikawa H: Regulatory T cells in cancer immunosuppression-implications for anticancer therapy. Nat Rev Clin Oncol 16: 356-371, 2019.
51. Lin X, Kang K, Chen P, Zeng Z, Li G, Xiong W, Yi M and Xiang B: Regulatory mechanisms of PD-1/PD-L1 in cancers. Mol Cancer 23: 108, 2024.
52. Sabit H, Arneth B, Abdel-Ghany S, Madyan EF, Ghaleb AH, Selvaraj P, Shin DM, Bommireddy R and Elhashash A: Beyond cancer cells: How the tumor microenvironment drives cancer progression. Cells 13: 1666, 2024.
53. Tie Y, Tang F, Wei YQ and Wei XW: Immunosuppressive cells in cancer: Mechanisms and potential therapeutic targets. J Hematol Oncol 15: 61, 2022.
54. Jechorek D, Haeusler-Pliske I, Meyer F and Roessner A: Diagnostic value of syndecan-4 protein expression in colorectal cancer. Pathol Res Pract 222: 153431, 2021.
55. Zeng Y, Luo Y, Zhao K, Liu S, Wu K, Wu Y, Du K, Pan W, Dai Y, Liu Y, *et al*: m6A-mediated induction of 7-dehydrocholesterol reductase stimulates cholesterol synthesis and cAMP signaling to promote bladder cancer metastasis. Cancer Res 84: 3402-3418, 2024.
56. Palumbo JS and Degen JL: Mechanisms linking tumor cell-associated procoagulant function to tumor metastasis. Thromb Res 120 (Suppl 2): S22-S28, 2007.
57. Ricklin D, Hajishengallis G, Yang K and Lambris JD: Complement: A key system for immune surveillance and homeostasis. Nat Immunol 11: 785-797, 2010.
58. Monteith GR, McAndrew D, Faddy HM and Roberts-Thomson SJ: Calcium and cancer: Targeting Ca2+ transport. Nat Rev Cancer 7: 519-530, 2007.
59. Zhao H, Wu L, Yan G, Chen Y, Zhou M, Wu Y and Li Y: Inflammation and tumor progression: Signaling pathways and targeted intervention. Signal Transduct Target Ther 6: 263, 2021.
60. Ahrberg Y, Dallmann J, Freitag J, Hassan A, Jung C, Kiefer J, Muralidharan AM, Peter M and Beck JD: CIMT 2024: Report on the 21st annual meeting of the association for cancer immunotherapy. Hum Vaccin Immunother 20: 2381925, 2024.
61. Jiang P, Gu S, Pan D, Fu J, Sahu A, Hu X, Li Z, Traugh N, Bu X, Li B, *et al*: Signatures of T cell dysfunction and exclusion predict cancer immunotherapy response. Nat Med 24: 1550-1558, 2018.

62. Kang K, Xie F, Wu Y, Han C, Bai Y, Long J, Lian X and Zhang F: Genomic instability in lower-grade glioma: Prediction of prognosis based on lncRNA and immune infiltration. Mol Ther Oncolytics 22: 431-443, 2021.
63. Han H, Su H, Lv Z, Zhu C and Huang J: Identifying MTHFD1 and LGALS4 as potential therapeutic targets in prostate cancer through multi-omics mendelian randomization analysis. Biomedicines 13: 185, 2025.
64. Hui Y, Leng J, Jin D, Wang G, Liu K, Bu Y and Wang Q: BRG1 promotes liver cancer cell proliferation and metastasis by enhancing mitochondrial function and ATP5A1 synthesis through TOMM40. Cancer Biol Ther 25: 2375440, 2024.
65. Tadic S and Martínez A: Nucleic acid cancer vaccines targeting tumor related angiogenesis. Could mRNA vaccines constitute a game changer? Front Immunol 15: 1433185, 2024.
66. Kubota Y, Han Q, Aoki Y, Masaki N, Obara K, Hamada K, Hozumi C, Wong ACW, Bouvet M, Tsunoda T and Hoffman RM: Synergy of combining methionine restriction and chemotherapy: The disruptive next generation of cancer treatment. Cancer Diagn Progn 3: 272-281, 2023.
67. Qiu Y, Xie E, Xu H, Cheng H and Li G: One-carbon metabolism shapes T cell immunity in cancer. Trends Endocrinol Metab 35: 967-980, 2024.
68. Pereira JA, Lanzar Z, Clark JT, Hart AP, Douglas BB, Shallberg L, O'Dea K, Christian DA and Hunter CA: PD-1 and CTLA-4 exert additive control of effector regulatory T cells at homeostasis. Front Immunol 14: 997376, 2023.
69. Xiao B, Li G, Gulizeba H, Liu H, Sima X, Zhou T and Huang Y: Choline metabolism reprogramming mediates an immunosuppressive microenvironment in non-small cell lung cancer (NSCLC) by promoting tumor-associated macrophage functional polarization and endothelial cell proliferation. J Transl Med 22: 442, 2024.
70. Li Z, Ke H, Cai J, Ye S, Huang J, Zhang C, Yuan M, Lan P and Wu X: MTHFD1 regulates autophagy to promote growth and metastasis in colorectal cancer via the PI3K-AKT-mTOR signaling pathway. Cancer Med 13: e70267, 2024.
71. Zhang X and Wang Z: Targeting SHMTs and MTHFDs in cancer: Attractive opportunity for anti-tumor strategy. Front Pharmacol 15: 1335785, 2024.
72. Groth M, Moissiard G, Wirtz M, Wang H, Garcia-Salinas C, Ramos-Parra PA, Bischof S, Feng S, Cokus SJ, John A, *et al*: MTHFD1 controls DNA methylation in Arabidopsis. Nat Commun 7: 11640, 2016.
73. Manjili MH and Butler SE: Role of tregs in cancer dormancy or recurrence. Immunol Invest 45: 759-766, 2016.
74. Hoffmann F, Franzen A, de Vos L, Wuest L, Kulcsár Z, Fietz S, Maas AP, Hollick S, Diop MY, Gabrielpillai J, *et al*: CTLA4 DNA methylation is associated with CTLA-4 expression and predicts response to immunotherapy in head and neck squamous cell carcinoma. Clin Epigenetics 15: 112, 2023.
75. Grant CE, Flis AL, Toulabi L, Zingone A, Rossi E, Aploks K, Sheppard H and Ryan BM: DRD1 suppresses cell proliferation and reduces EGFR activation and PD-L1 expression in NSCLC. Mol Oncol 18: 1631-1648, 2024.